

## Author's Response to Anonymous Referee #2

Manuscript Number: cp-2017-112

5

Manuscript Title: Arc volcanism, carbonate platform evolution and palaeo-atmospheric CO<sub>2</sub>:  
Components and interactions in the deep carbon cycle

### General Comments by Anonymous Referee #2:

10 Referee comment:

This is an interesting study that explores links between arc activity and the long-term CO<sub>2</sub> budget. This is not a new effort, as the authors acknowledge, but the authors apply a statistically rigorous method that most reliably tests the relationships between two signals, subduction zone length and atmospheric CO<sub>2</sub>. This manuscript is also very well written and constructed. That said, I do have a few concerns on the  
15 data compilation, methodology, and the interpretations. I do not have a good grasp of wavelet analyses used in this paper, so I would not comment on the methodology. However, I understand that the conclusions are based on the reconstruction and data compilations.

The study is partially inspired by the hypothesis in Lee et al. papers. I notice that “continental arc” in Lee et al. is not equivalent to “CIA” in this study, because thickened crusts lead to evolved magma that  
20 is more efficient in wall rock decarbonation when intruding.

Author response:

*We originally differentiate the ‘continental arc’ in the Lee et al. (2013) and Cao et al. (2017) papers from our work with the term ‘carbonate intersecting arc [CIA],’ which was defined to capture the  
25 entire contribution of decarbonation and the release of CO<sub>2</sub> into the atmosphere along subduction zones. As Cao et al. (2017) are quantifying only volcanic CO<sub>2</sub> along continental arcs, to call our subduction zone measurements a surrogate for ‘arc activity’ is no longer appropriate. This is because our estimations of subduction zone lengths capture a greater source of CO<sub>2</sub> than arc volcanism alone, including diffuse degassing from crustal magmatic processes. As such, we have redefined the  
30 terms ‘carbonate-intersecting continental [CIC] subduction zones’ and ‘non-carbonate-intersecting continental [non-CIC] subduction zones,’ which are complementary and together make up global subduction zones (pg. 3, lines 11-13).*

Referee comment:

35 It is good that the authors did not extract CO<sub>2</sub> signals from models like GEOCARB, so did not mix model results with the data extracted from natural samples. In addition to the uncertainty issues noted by the authors, GEOCARB scales tectonic input of CO<sub>2</sub> to the spreading rate of mid-ocean ridges, so does not explicitly account for magmatic-metamorphic outgassing at arcs. Although faster MOR spreading in general corresponds to more vigorous global tectonics, arc activities also depend on the  
40 configuration of plates. Thus, it is logically inconsistent to compare arc lengths with GEOCARB model results. The authors apply a filter to remove high-frequency noises (note: “noise” might not perfectly

appropriate in this context), but I doubt whether the resolution and uncertainties in ages of Park and Royer data are within a few million years. I suggest that the authors briefly summarize and discuss both uncertainties and temporal resolution of the data compilation of Park and Royer (2011).

5 Author response:

***In accordance with the referee's suggestion, the uncertainties in the Park and Royer (2011) compilation were summarised (pg. 23, lines 24-27).***

Referee comment:

10 I have a major concern on the accumulation model used in this study. Early Paleozoic and pre-Cambrian carbonate platform deposits are entirely ignored in the reconstruction, so the CIA curve (Fig. 4) starts at 0 km at 410 MA, which is unrealistic. The CIA lengths almost monotonically increase, and the present CIA length is about 6 times of Permian and 1.5-1.2 times of Cretaceous. This curve alone, without any wavelet analyses, would falsify the hypothesis of Lee et al., misleading the readers to conclude that the  
15 contribution of arc activity to Earth's long-term climate is minimal.

Author response:

***We agree with the referee regarding the construction of the Accumulation Model. It was originally designed to exhibit the evolution of carbonate platforms to cover the timeframe of the plate tectonic reconstructions, and so only included all platforms back to 410 Ma. This has been corrected in the current model, which includes Ordovician and Silurian platforms as hypothesised by Kiessling et al. (2003). Reference is made to the creation of this model with the earlier Paleozoic platforms (pg. 5, lines 16, 22-24). We would like to note that the CIC subduction zone curve (previously referred to as the CIA curve) did not start from 0 km, but from 3140 km. It is noted that in the new model, CIC  
25 subduction zone lengths are estimated to be 7940 km in length at 410 Ma (pg. 17, line 8-9).***

Referee comment:

As the authors have noted, the accumulation model provides an upper bound because it is assumed that the platform carbonate was not depleted in geologic events (erosion, subduction etc.). It is only fair to  
30 compare the arc lengths with CO<sub>2</sub> proxies if the authors also provide a lower bound estimate.

Author response:

***To create a lower bound estimate would mean creating a model where one can reasonably assume that carbonate platforms have been depleted over time. We attempted a model like this, where  
35 carbonate platforms were actively interacting with subduction zones only in the geological period within which they were produced, based on the Kiessling et al. (2003) compilation (Figs. R1, R2). This lower bound estimate model assumed that older, buried carbonate platforms were depleted or 'inactive', and were not interacting with arc magmatism. The results indicated that the spatial area of carbonate platforms in this model was consistently lower than the Accumulation Model (Fig. R1),  
40 and implied that carbonate platforms produced in the past are no longer significant reservoirs in the present (Fig. R2). We found these results and the assumption of fast depletion to be unrealistic. This is especially true because the carbonate platforms mapped by Kiessling et al. (2003) are currently in***

*existence, and it is not known how carbonate platform carbon contents have depleted through time. While we agree that a lower bound estimate is useful, it is not possible to create one for the past 410 Ma with the data set we are working with. Instead, we state that we are providing a first-pass approximation based on a set of assumptions that are clearly defined.*

5

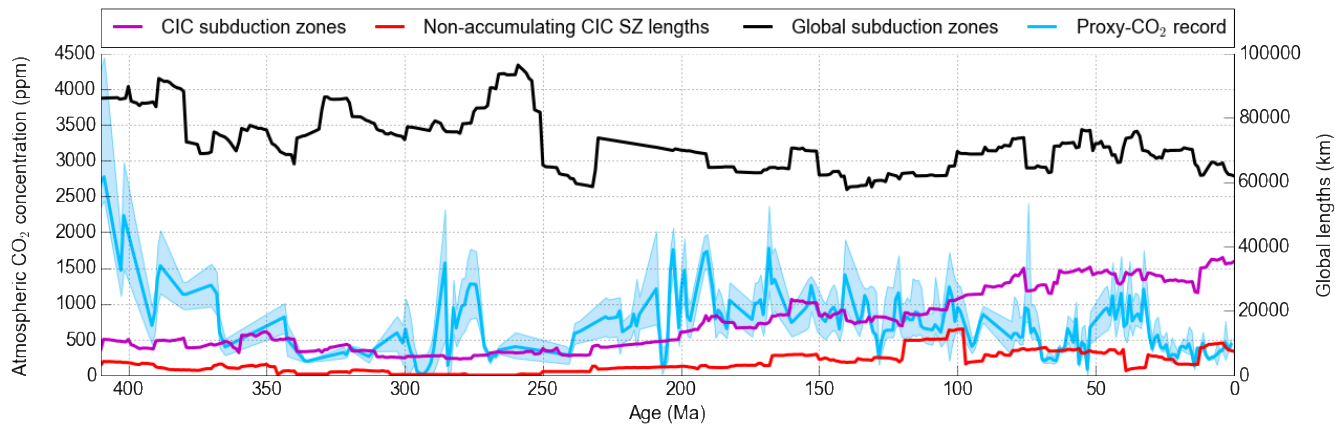


Fig R1. Total global lengths of subduction zones (black) compared with CIC subduction zones (magenta) which is included in our manuscript, and our lower bound estimate of non-accumulating CIC subduction zone lengths (red).

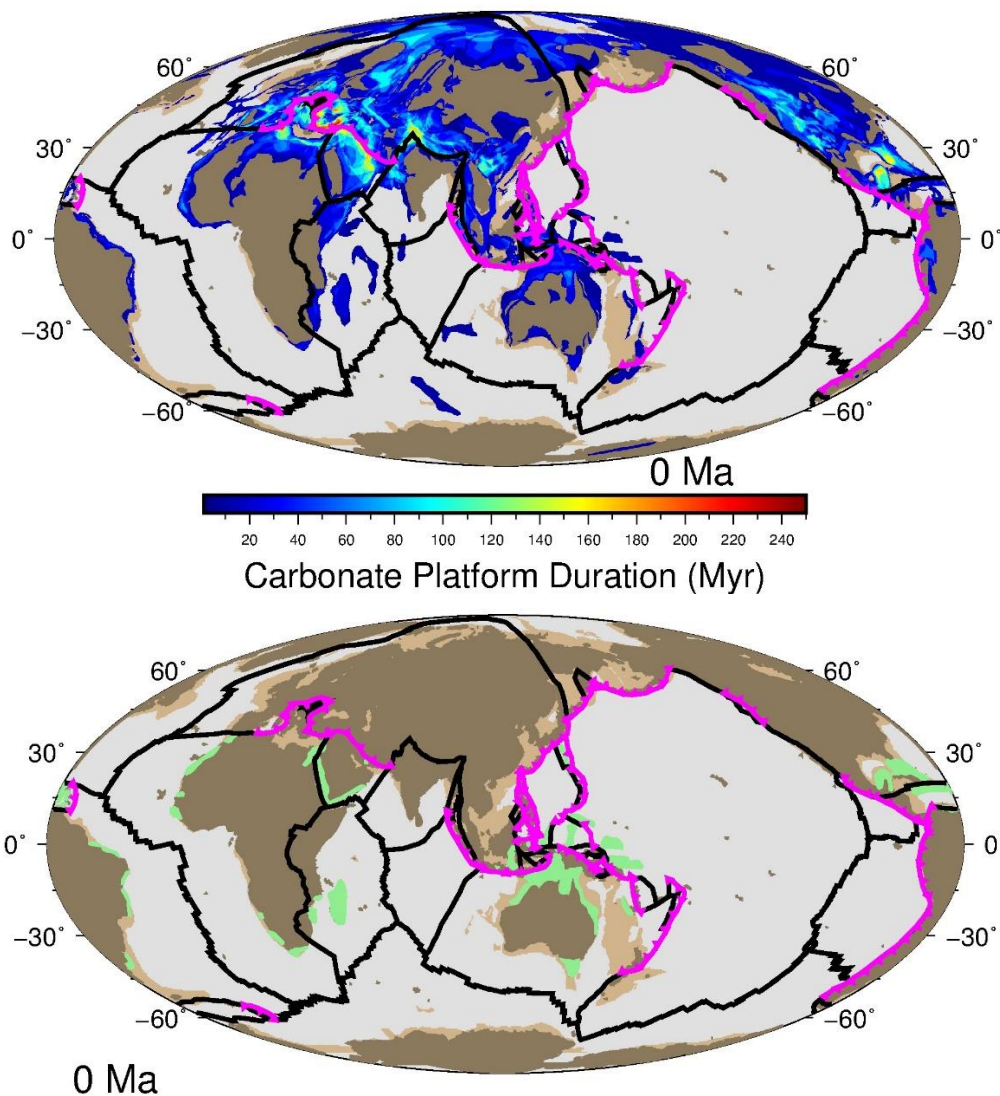


Fig R2. Plate reconstructions with plate boundaries (black), subduction zones (purple) and distribution of carbonate platforms in the Accumulation model (upper) and in the lower bound estimate model (lower). The colour bar corresponds to the duration of time that the carbonate platforms were actively developing in the crust.

Referee comment:

The CIA and NCIA lengths are derived from the GPlates reconstruction and 24 palaeo graphic maps. It is not clear to me how the authors differentiate arc lengths from lengths of convergent margins, or subduction versus collision zones. Again, it will help the readers to assess the quality of reconstruction if uncertainties are discussed in addition to the model assumptions and limitations. In the current version it sounds a bit like almost no error!

Author response:

5 *We attempt to make our analysis clearer by redefining lengths of ‘carbonate-intersecting continental [CIC] subduction zones’ and ‘non-CIC subduction zones,’ (pg. 4, lines 4-7). We are not solely concerned with volcanic CO<sub>2</sub> emissions but rather the combination passive (diffuse) and active CO<sub>2</sub> emissions along all subduction zones, and so we believe that we no longer need to differentiate the types of convergent margins.*

Referee comment:

10 The authors need to justify that the data and model reach a 1-Myr resolution (Line 7, Page 26).

Author response:

15 *While we cannot find where the referee is pointing to on page 26, reference to the 1 Myr resolution of our model is made on pg. 4, lines 20-21. The key components are carbonate platforms that are assumed to be active over a segment of geological time in the Kiessling et al. (2003) compilation. These are linked to plate reconstructions that provide evolving plate boundaries in 1 Myr intervals, thus allowing us to track the subduction zone and carbonate platform interactions at finer temporal resolutions than the original Kiessling et al. (2003) snapshots.*

20

Referee comment:

25 The present global length of CIA in Figure 4 is about 35,000 km, more than double of the lengths of continental arcs measured from geologic maps (15,000 km; Fig. 4d in Cao et al., 2017 EPSL). This large discrepancy makes me worry about the GPLates reconstruction in this study. Where does the extra CIA length account for? It is essential to address this discrepancy in the revised manuscript for the readers to understand the meaning of CIA defined in this study.

Author response:

30 *The Cao et al. (2017) approach is very different to our approach in the way that it compiled arc volcanics from active margins. For plate tectonic reconstructions, one can have a subduction zone and produce very little arc volcanism (e.g., southern Turkey, parts of the Andean margin, etc. – see figure below), while we know that tectonic convergence and subduction is occurring. That subduction is carrying volatiles into the mantle wedge, with partial melting likely being trapped in the crust (rather than being extruded) to produce more diffuse CO<sub>2</sub> emissions. In essence, the Cao et al. (2017) work provides a minimum length of continental volcanic arcs (largely because it relies on comprehensive sampling and preservation of volcanic rocks), while our work represents a likely upper bound on continental arc lengths.*

35

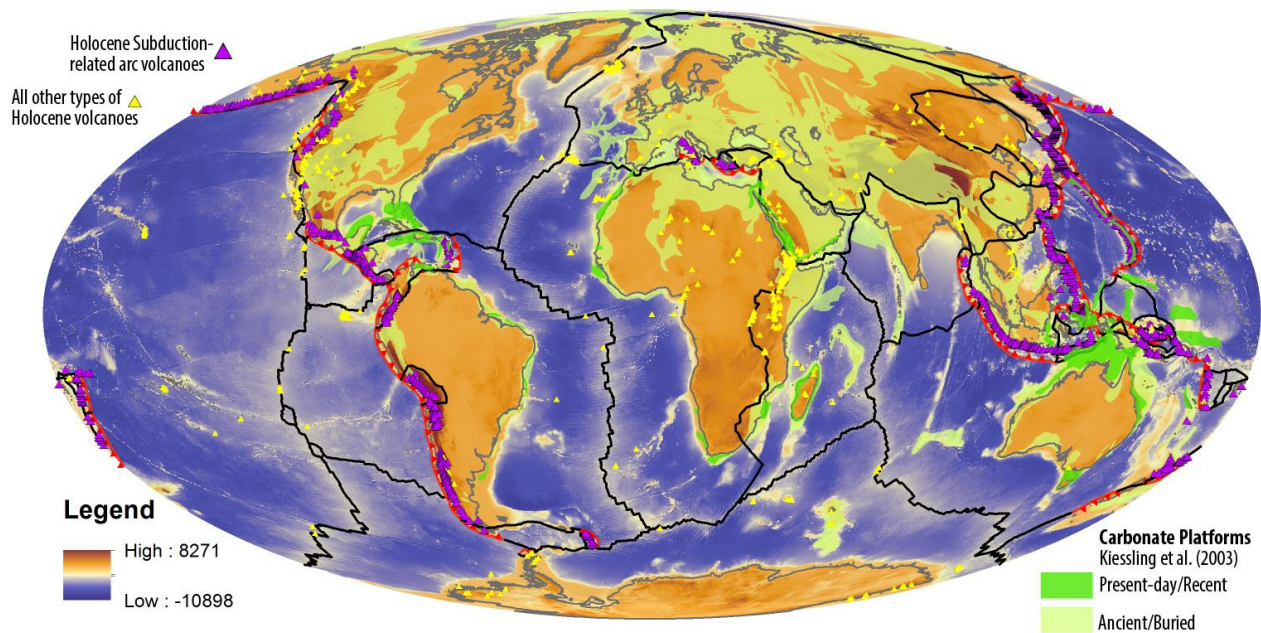


Fig R3. Present-day subduction zones (red) from Bird et al. (2003), compared with Holocene volcanism related to subduction (purple) or other tectonic settings (yellow). The active (bright green) and buried (light green) carbonate platforms from Kiessling et al. (2003) are also plotted.

5



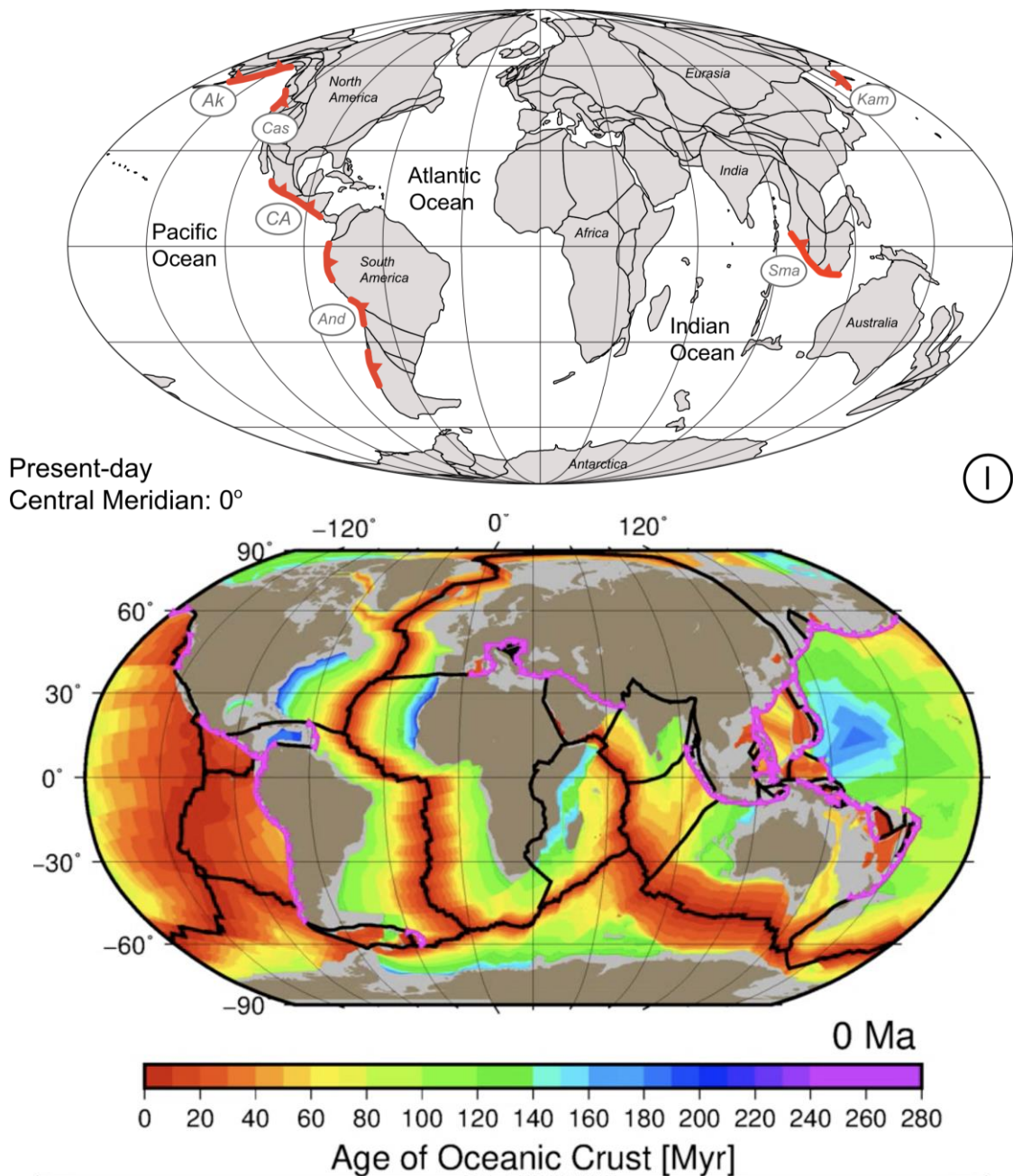


Fig R4. Present-day continental arcs (red lines) from Cao et al. (2017) [left] and present-day oceanic and continental subduction zones (magenta lines) from the GPlates reconstructions used in this study [right]. The obvious differences include that we treat the Mediterranean (e.g. parts of Italy, etc.) and much of east Asia (e.g. Japan) as continental arcs, unlike in Cao et al. (2017). Intra-oceanic subduction zones are not used in our study.

Referee comment:

5 I am extremely curious to know how wavelet analysis using the compilation of Cao et al. (2017) or McKenzie et al. (2017) and the CO<sub>2</sub> record (Park and Royer, 2011) would turn out. It is not clear to me how arcs on subducted fossil plates are constructed in GPlates or whether this portion of fossil arc (subduction zone) is added in Fig. 4. This is not directly relevant to the conclusion of this study, but the authors should state the assumptions and protect their model results from being misinterpreted.

Author response:

10 ***Applying the analysis to the Cao et al. (2017) material is a significant undertaking, largely because the subduction zones are plotted on single snapshots (representing longer geological timeframes) on an entirely different plate reconstruction. This is outside the scope of this work, but should be a component of future work.***

15 Referee comment:

I don't think it is a good idea to mix all decarbonation processes at convergent margins in Section 5.3. These are not the limitations of THIS model that addresses the relationship between arcs and long-term CO<sub>2</sub>. Instead, the authors might focus on a series of assumptions and limitations in the reconstruction and data compilation (comments above).

20

Author response:

25 ***As the referee mentions, there is very little work that has been done on disambiguating the decarbonation processes at subduction zones. While some modelling work has been undertaken (e.g. Gonzales et al., 2016) it is difficult to distinguish the contribution of crust from subducting sediments, and the relative contribution of other factors including the angle and thickness of the subducting slab. As such, we are forced to make a simplistic assumption that subduction zone lengths are correlated with CO<sub>2</sub> emissions in our analysis, and subsequently make our assumptions and limitations clear to the readers (Section 2.2, pg. 7-8; Section 5.3, pg. 25-26 ).***

30

Referee comment:

To address these concerns, it potentially requires substantial work of model development and data compilation and it seems that this will take long. That is why I suggest rejection but with strong encouragement to resubmit. I hope the authors are willing to perform a major revision, as it will significantly strengthen their arguments. I would like to say that I have great respect for the work that has been done in this project and for this research group in general, but I cannot be positive at this time. I very much hope that my comments help to improve the manuscript.

35

General comments by the authors:

40 1. All instances of CIA and NCIA lengths have been changed to CIC and non-CIC subduction zone lengths respectively.



2. Basic assumptions about the CO<sub>2</sub> emissions at subduction zones have been redefined and stated (pg. 1, line 3-7; pg. 3, line 9-11, 27-28; pg. 4, line 1-2, section 2, pg. 8, Section 2.4; ).
3. As per suggestion by Referee #2 and the Editor, the inclusion of Ordovician and Silurian Carbonate Platforms has been made to the Accumulation Model, which has been stated in the manuscript (pg. 5, Section 2.1).
4. Assumptions and limitations of the Accumulation Model (pg. 6-7, Section 2.2; pg. 24-25, Section 5.3) and wavelet analysis (pg. 22, line 24-27) have been re-written to better describe the limitations of our single-estimate model.
5. Results, discussion and figures have been updated to reflect new analyses (pg. 11-22).

Author response:

***General comments by the referee have all been accepted and adapted into the text. Further changes to the manuscript include:***

- 1. Conducting our analysis again and replacing all figures in the text (Figs. 1-5 and S1-S2) and re-writing the results and discussion to reflect new and different results (Section 4).***
- 2. Changing the title to change the focus from volcanic arcs to the broader interactions between active margins and crustal carbonate platforms.***
- 3. Changing all instances of 'CIA lengths' to 'CIC subduction zone lengths,' including within figures and captions.***
- 4. Specifying why it is difficult to test the hypothesis of Lee et al. (2013) (pg.3, lines 20-21).***
- 5. Streamlining text for word economy and comprehension, e.g. pg. 4, line 9.***
- 6. Elaborating on the work by Cao et al. (2017) in comparison to our work (pg. 4, lines 9-15).***
- 7. Explaining our plate reconstruction in more detail (pg.5, lines 2-14), and our process of measuring subduction zone lengths (pg. 9, lines 6-15).***

# Are volcanism Subduction zone and, carbonate platform evolution interactions since the Devonian and palaeo-atmospheric CO<sub>2</sub>: influence on Components and interactions palaeo-atmospheric CO<sub>2</sub> in and the deep carbon cycle

5 Jodie Pall<sup>1</sup>, Sabin Zahirovic<sup>1</sup>, Sebastiano Doss<sup>1</sup>, Rakib Hassan<sup>1,2</sup>, Kara J. Matthews<sup>1,3</sup>, John Cannon<sup>1</sup>, Michael Gurnis<sup>4</sup>, Louis Moresi<sup>5</sup>, Adrian Lenardic<sup>6</sup> and R. Dietmar Müller<sup>1</sup>

<sup>1</sup>EarthByte Group, School of Geosciences, University of Sydney, NSW 2006, Australia.

<sup>2</sup>Geoscience Australia, GPO Box 378, Canberra- 2601, ACT, Australia.

<sup>3</sup>Department of Earth Sciences, University of Oxford, Oxford, OX1 3AN, UK.

10 <sup>4</sup>Seismological Laboratory, California Institute of Technology, California 91125, USA.

<sup>5</sup>School of Earth Sciences, University of Melbourne, Victoria 3010, Australia.

<sup>6</sup>Department of Earth Science, Rice University, Texas 77005, USA.

*Correspondence to:* Jodie Pall (jodierae.pall@gmail.com)

## **Abstract**

15 The CO<sub>2</sub> liberated along continental subduction zones through volcanism intrusive/extrusive magmatic activity and the resulting active and diffuse -outgassing influences global atmospheric CO<sub>2</sub>. However, when continental melts derived from continental subduction zones intersect buried carbonate platforms, decarbonation reactions may cause the contribution to atmospheric CO<sub>2</sub> to be far greater than non-intersecting parts of segments of the active margin that lacks buried carbon-rich rocks and carbonate platforms subduction zones. Carbon dioxide (CO<sub>2</sub>) liberated at arc volcanoes that intersect buried carbonate platforms plays a larger role in influencing atmospheric CO<sub>2</sub> than those active margins lacking buried carbonate platforms. This study investigates the contribution of carbonate-intersecting continental (CIC) subduction zones of carbonate-intersecting arc activity on to palaeo-atmospheric CO<sub>2</sub> levels over the past 410 million years by integrating a plate motion and plate boundary evolution model with an evolving carbonate platform development model through time. Our modelled subduction zone lengths and carbonate intersecting arc lengths approximate arc activity with time, and can be used as input into fully-coupled models of CO<sub>2</sub> flux between deep and shallow reservoirs.

20

25

Continuous and cross-wavelet analyses as well as wavelet coherence analyses were used to evaluate trends between the evolving lengths of CIC subduction zones, non-CIC subduction zones and total global subduction zones, and are examined for periodic, linked behaviour with carbonate intersecting arc activity, non-carbonate intersecting arc activity and total global subduction zone lengths and the proxy-  
5 CO<sub>2</sub> record between 410 Ma and the present. Wavelet analysis revealed significant linked periodic behaviour between 75-50 Ma, where CIC subduction zone lengths are global-carbonate intersecting arc activity is relatively high and are correlated with ~~where~~ peaks in palaeo-atmospheric CO<sub>2</sub> ~~is correlated with peaks in global-carbonate intersecting arc activity~~, characterised by a ~32 Myr periodicity and a 10 Myr lag of CO<sub>2</sub> peaks following CIC subduction zone length peaks ~~after carbonate intersecting arc length~~  
10 peaks. The linked behaviour may suggest that the relative abundance of carbonate intersecting arcs ~~CIC subduction zones~~ played a role in affecting global climate during the Late Cretaceous to Early Palaeogene greenhouse. At all other times, atmospheric CO<sub>2</sub> emissions from carbonate intersecting arcs ~~CIC subduction zones~~ ~~were~~ are not well correlated with the proxy-CO<sub>2</sub> record. Our analysis of reconstructed carbonate platforms in relation to continental subduction zones ~~did~~ does not support the idea that  
15 carbonate intersecting arcs ~~CIC subduction zone~~ activity is more important than non-carbonate intersecting ~~CIC arcs~~ subduction zone activity in driving changes in palaeo-atmospheric CO<sub>2</sub> levels. This suggests that the carbon fluxes from subduction zones and carbonate platform intersections ~~tectonic controls~~ ~~are more elaborate than the subduction-related volcanic emissions component~~ what is modelled ~~time-varying or~~ and that other feedback mechanisms between the geosphere, atmosphere and  
20 biosphere likely played larger-dominant roles in modulating climate in throughout the Phanerozoic since the Devonian. Our modelled subduction zone lengths and carbonate-intersecting arc lengths approximate arc magmatic activity ~~with~~ through time, and can be used as input into fully-coupled models of CO<sub>2</sub> flux between deep and shallow carbon reservoirs.

## 1 Introduction

25 The current paradigm of the deep carbon cycle (i.e. the planetary cycling of carbon over million-year timescales) attributes fluctuations in the atmospheric carbon dioxide (CO<sub>2</sub>) to the realm of tectonic forces, where arc volcanic subduction-related emissions (van der Meer et al., 2014; Kerrick, 2001) and

metamorphic decarbonation (Lee et al., 2013) are major CO<sub>2</sub> sources, and the processes of silicate weathering (Sundquist, 1991; Kent and Muttoni, 2008) and marine organic carbon burial (Bernier and Caldeira, 1997; Ridgwell and Zeebe, 2005) are major sinks removing CO<sub>2</sub> from the atmosphere. Subduction plays a critical role in this cycle. In a dynamic interplay, oceanic lithosphere is consumed at subduction zones, removing carbon bound in pelagic carbonate seafloor sediments from the exogenic carbon cycle. Simultaneously, CO<sub>2</sub> is emitted through diffuse outgassing and during arc volcanism along subduction zones ~~and at mid-ocean ridges (MORs) where new oceanic crust is being created~~ (Burton et al., 2013; Keleman and Manning, 2015). Despite the proposal that silicate weathering has, at some stages, been a dominating control of atmospheric CO<sub>2</sub> levels (Kump, 2000; Kent and Muttoni, 2013), arc magmatism at icehouse-greenhouse transitions is thought to be the first-order control on climate fluctuations while silicate weathering acts to modulate atmospheric CO<sub>2</sub> as a secondary regulative process (Ridgwell and Zeebe, 2005; Lee and Lackey, 2015; McKenzie et al., 2016). Recent studies have found support for links between global arc activity and icehouse-greenhouse transitions using detrital zircon ages, modelling and experimental techniques, particularly as drivers of greenhouse conditions in the Cambrian (McKenzie et al., 2016; Cao et al., 2017), Jurassic-Cretaceous (McKenzie et al., 2016) and early Palaeogene (Lee et al., 2013; Carter and Dasgupta, 2015; Cao et al., 2017).

Recently, carbon and helium isotope analysis from modern volcanic arc gas has provided evidence that volcanic arcs that assimilate crustal carbonate in their magmas through decarbonation reactions have a greater atmospheric CO<sub>2</sub> contribution than other types of arcs (Mason et al., 2017). Modern crustal carbonate reservoirs are a result of global organic and inorganic carbonate production throughout the Phanerozoic, which has contributed to the build-up of expansive, shallow-water carbonate sequences including ramps and rimmed shelves along continental margins, hereafter referred to as 'carbonate platforms' (Kiessling et al., 2003). At different points in Earth's history, active (from extrusive volcanism) and passive (from intrusive magmatism) emissions from ~~continental~~ carbonate-intersecting arc continental (CIAs/CIC) subduction zones may have dominated global ~~volcanic carbon flux~~ carbon flux from subduction zones, such as during the Cretaceous (144-65 Ma) where continental arcs are hypothesised to have been longer than modern day lengths and where a greenhouse climate prevailed (Lee et al., 2013; van der Meer et al., 2014; Cao et al., 2017). It is plausible that at other points in Earth's

history, crustally-derived carbon ~~at other points in Earth's history~~ has played a significant role in affecting global climate, and that there may be a periodic trend in carbon released from continental arcs through time related to ~50 Myr flare-ups (Lee and Lackey, 2015) and continent assembly and dispersal which cause transitions from intraoceanic-arc- to continental-arc-dominated states (Lenardic et al., 2011; Lee et al. 2013). However, it is difficult to test this hypothesis, especially due to due to poor preservation of ancient intra-oceanic arc rocks ~~preservation bias in the geological record~~ (Berner, 2004).

This challenge is addressed using wavelet analysis, which attempts to detect correlations and periodicities in two time series at any scale or duration (Grinsted et al., 2004). Compared to other windowing techniques that find time-dependent correlations between two signals such as the windowed Fourier transform, the wavelet transform is preferable because it is localised (bounded) in both time and frequency, whereas Fourier transforms are only localised in frequency (Torrence and Compo, 1998). Hence, the wavelet transform can better constrain correlations in time and is better-suited than the Fourier transform to approximating data with sharp discontinuities, such as those addressed in this investigation.

We aim to investigate whether the CO<sub>2</sub> flux from CIC subduction zones ~~volcanic arcs that interact with buried carbonate platforms (CIA activity) are~~ significantly different to ~~volcanic arcs~~ the flux from subduction zones that do not intersect with buried carbonate reservoirs (~~non-carbonate intersecting are [NCIA] act~~ CIC activity) in influencing global palaeo-atmospheric CO<sub>2</sub> concentrations. Our study explores volcanic and passive outgassing of CO<sub>2</sub> along continental subduction zones ~~volcanic arc activity~~ as an aspect of the deep Earth carbon cycle using a combination of plate reconstruction software and wavelet analysis. Only Cao et al. (2017) and this study have endeavoured to ~~look beyond the use of~~ apply palaeogeographic maps to explore the distribution of continental arcs through space and time in a plate tectonic framework. However, the work by Cao et al. (2017) relies on discrete plate reconstruction snapshots, rather than the continuously evolving plate boundary evolution model applied here. In addition, Cao et al. (2017) compile arc volcanic products, which may be affected by preservation and sampling bias, and may not capture magmatic products trapped (deep) in the crust or those lost to erosion. The Cao et al. (2017) approach of estimating continental subduction zone lengths is therefore a lower-limit, while our approach is likely an upper limit of continental subduction zone lengths through time. Furthermore,

wavelet analysis is used to deconvolve two time series at a time (e.g. our [CIC and non-CIC subduction zone](#) ~~CIA and NCIA~~ lengths with the palaeo-atmospheric CO<sub>2</sub> record by Park and Royer [2011]) to uncover any periodicities or correlations. With a plate [motion](#) model that extends to 410 Ma, we ~~model track~~ space-time trends of global subduction zone and carbonate platform interactions since the Devonian (410 Ma), ~~where subduction zone lengths are used as a surrogate measure for volcanic arc lengths.~~ This paper is accompanied by an open-source ‘subduction zone analysis toolkit’ (Doss et al., 2016) to help enable the use of digital plate motion models (e.g. Matthews et al., 2016) and other tools to investigate aspects of the deep carbon cycle.

## 2 Modelling ~~global arc activity~~ [subduction zones](#) and [carbonate platform](#) evolution

We investigate the combined effect of [evolving global subduction zone lengths](#) and the subsequent decarbonation of crustal carbonates by ~~arc magmas~~ [subduction zone melts](#) to create a first-order approximation of the contribution of [CO<sub>2</sub> outgassed at carbonate-intersecting arc volcanism](#) ~~CIC~~ [carbonate-intersecting continental \(CIC\) subduction zones](#) to palaeo-CO<sub>2</sub> levels over the past 410 Myr. An ‘Accumulation Model’ of carbonate platform evolution was produced to represent the long-term persistence and build-up of carbonate platforms in upper continental crust. ~~Global subduction zone lengths are used as a surrogate for global volcanic arc lengths through time, where we assume a general correspondence of arc lengths to volcanic activity.~~ [The plate reconstructions used in this study have been developed through a synthesis of marine and continental geological and geophysical data, including seafloor spreading histories for the post-Pangea timeframe \(Seton et al., 2012; Muller et al., 2016\), and largely paleomagnetic and continental geological constraints for pre-Pangea times \(Domeier and Torsvik, 2014; Matthews et al., 2016\).](#) Continental subduction zones are implemented where the geological record indicates [arc volcanism or intrusive magmatism, an active accretionary melange, active orogens associated with subduction zones, formation of supra-subduction zone ophiolites, and other indicators of an active margin.](#) As our plate reconstructions are global, plate boundary evolution requires [continuously evolving topological polygons to capture plate motions \(Gurnis et al., 2012\), meaning that subduction zones are implemented along entire convergent margins, rather than only where](#)



5 preserved arc volcanics are found. Our plate reconstructions that include continental motions and plate boundary evolution are available as open-access community resources (<https://www.earthbyte.org/global-plate-models/>). Using open-source and cross-platform plate reconstruction software GPlates (<http://gplates.org/download.html>) and a new pyGPlates Python application programming interface (API) (<https://www.gplates.org/docs/pygplates/>), we measure the length of subduction zones at 1 Myr intervals since 410 Ma and track the length of subduction zones that interact with interaction between subduction zones and major carbonate platforms (CIC subduction zones), typically occurring on continents, as well as the length of subduction zones that do not intersect carbonate platforms (non-CIC subduction zones), and total global subduction zone  
10 lengths through time to better understand the effect of outgassing along subduction zones carbonate intersecting arc magmatism on palaeo-CO<sub>2</sub> and palaeoclimates interpreted from proxy data (Park and Royer, 2011).

## 2.1 An ‘Accumulation’ model of carbonate platform development

15 Palaeogeographic maps of carbonate platforms spanning the Phanerozoic since the Ordovician from Kiessling et al. (2003) were used to assemble a model of a time-dependent evolution of carbonate platform accumulation through time. The ~~twenty-four~~<sup>31</sup> maps represent the spatial extent of carbonate platforms at the maximum marine transgression within each epoch for the Phanerozoic (Kiessling et al., 2003). The carbonate platform geometries were georeferenced to geographic WGS84 co-ordinates in ArcGIS (ESRI, 2011) to be compatible with GPlates, the open-source plate reconstruction software (Boyden et al., 2011).  
20 A GPlates file was created to depict evolving carbonate platform development accumulation from 410 Ma to present-day using platforms existing since the Ordovician, in order to better capture buried carbonate platforms at the beginning of the model timeframe. Creating this model involved stitching together ~~twenty-four~~<sup>all</sup> carbonate platform shapefiles and allowing them to persist until present day. Ages had been ascribed based on the, where reef patterns in each epoch had been adjusted to the Golonka and  
25 Kiessling (2002) Phanerozoic timescale. However, owing to new chronostratigraphic data, the geological times ascribed to the existence of carbonate platforms in each epoch were converted to the corresponding times in the latest chronostratigraphic scheme given in the 2016 version of the International Stratigraphic

Chart (Cohen et al., 2013). Subsequently, the static carbonate platform shapefiles were reconstructed with the rotations and plate geometries associated with an older plate [motion](#) model (Scotese, 2016), similar to the model used by Kiessling et al. (2003). In GPlates, the carbonate platform geometries were assigned Plate IDs based upon their overlapping position within the reconstructed continental geometry.

- 5 Carbonate platforms were rotated to their present-day positions, and Plate IDs associated with the Scotese (2016) model were translated into corresponding Plate IDs from the Matthews et al. (2016) plate motion model. By obtaining the present-day geometry of the ancient carbonate platforms, attaching these geometries to any other plate motion model becomes straightforward. The evolving carbonate platform model was created by layering each carbonate platform geometry such that it persists to present-day.
- 10 ‘Accumulation’ Model we implement in this study embodies the idea that carbonate platforms accumulate in crustal reservoirs through time.

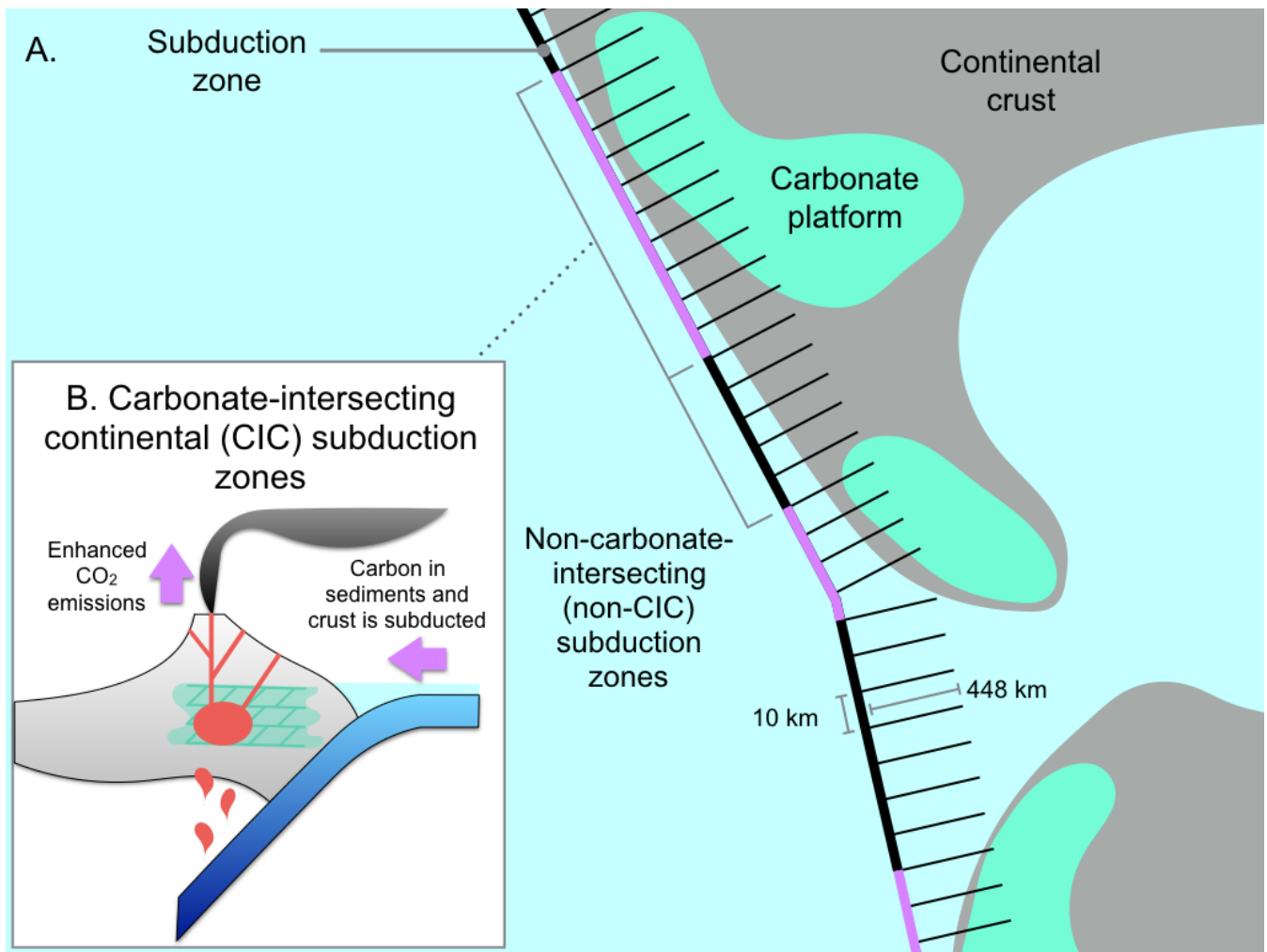


**Figure 1:** (A) Schematic representation of the ~450-km-long cross-profile ‘whiskers’ that were constructed along subduction zones (purple and black) spaced 10 km apart in the direction of subduction. At regular intervals along the whiskers, the carbonate platform grid on the overriding plate was sampled where carbonate polygons have a value of 1, and everywhere else is zero. If the whisker intersects with a carbonate platform, it represents 10 km along a carbonate-intersecting volcanic arc. (B) Schematic representations of carbonate-intersecting continental arcs. Carbonate platforms become buried over time, forming reservoirs in the crust. Through assimilation and decarbonation reactions, arc magmas interact with upper-crustal carbonates and liberate significantly more CO<sub>2</sub> emissions than at non-intersecting continental arcs.

## 2.2 Assumptions and limitations of the Accumulation Model

10 The Accumulation Model is an end-member scenario of how carbonate platforms evolve through time. Carbonate accumulation is assumed to accrete onto continental margins and persist as mid-crustal carbonate reservoirs from the time of their deposition-formation to the present (Fig. 1). Ancient carbonate platforms are known to persist to present-day in surface reservoirs, and can be reconstructed from the

geological record as they either outcrop, are sampled by drilling or are interpreted from seismic reflection studies (Kiessling et al., 2003). Some crustal carbonate is inevitably eroded or subducted into the deep mantle, however it is improbable that most reservoirs have been destroyed in ~~the~~this way as most carbonate platforms accumulate on continental margins and are not likely to subduct (Lee and Lackey, 5 2015). Given limited erosion on passive continental margins, except in the cases of major uplift and deformation through mountain-building, it is far more likely that carbonate platform ~~expansion~~accretion has exceeded their depletion by erosion or consumption through time (Ridgwell and Zeebe, 2005). Moreover, the existence of fossil reef data as far back as the ~~Ordovician-Precambrian~~ (~~Kiessling et al., 2003~~Grotzinger and James, 2000) favours the notion that extensive portions of platforms have been well-10 preserved in continents.

Nevertheless, our model assumes that carbonate platforms  
~~Since our model is temporally limited in the Phanerozoic from the Devonian to present day, it suggests that carbonate are intersections would have increased through time, which is likely an oversimplification of the carbonate depositional process on continental margins. In addition, since the accumulation rate of carbonate platforms is variable in both space and time, we apply a simplistic Boolean assumption (i.e. a carbonate platform is likely to persist in the sedimentary record, with an unknown thickness).~~15

~~A significant limitation of the Accumulation Model is that we assume carbonate platforms have not been significantly depleted by sustained ~~volcanic-mantle-crust~~ interaction through time. We follow this assumption because there is no way to account for their rate of depletion given the complexity of inter-20 dependent factors such as platform thickness, heat, pressure, composition and the duration of interaction (Johnston et al., 2011). Accounting for the thickness of platforms and the depletion of reservoirs over time are areas of necessary future developments in the model.~~

We accept that our Accumulation Model is a simplification of the carbonate reservoir system and may lead to an overestimation of CIC subduction zone lengths. However, this may be a reasonable proxy for 25 the substantial amount of CO<sub>2</sub> emitted via diffuse outgassing that is largely un-accounted for in global estimates of carbon emitted at continental arcs (fore-arc, arc and back-arc settings) (Keleman and Manning, 2015). Given little evidence of carbon storage in arc crust, ~~these estimates~~these estimates provide

important information, if not an upper-bound estimate, of degassing from CIC subduction zones which are hypothesised to be a significant source of atmospheric CO<sub>2</sub> (Keleman and Manning, 2015).

While some Precambrian carbonate platforms are known to exist have been described (Grotzinger and James, 2000), no effort has yet been made to map their occurrence globally, and thus only those captured

5 in the Kiessling et al. (2003) biogeographic maps ~~were~~ could be incorporated into our Accumulation Model. While it is expected that accounting for Precambrian platforms would not drastically change the analysis, this model nevertheless represents a degree of underestimation of the crustal carbonate reservoir.

The model also does not account for the subduction of some carbonate platforms over the past 410 Ma, although it is expected that accounting for this would not drastically change the results. Finally, because  
10 subduction of carbonate platforms is not considered, the Accumulation Model provides an upper bound of carbonate arc interactions. However, this may be a reasonable proxy for the role of subducted carbonate platforms that would contribute substantial volatiles into the mantle wedge above a subducting slab.

### **2.3 Measuring global subduction zone lengths with pyGPlates**

We use the open access global plate motion model from Matthews et al. (2016) to analyse the spatio-  
15 temporal distribution of subduction zone volcanic arcs in a deep-time tectonic framework and test the hypothesis that subduction zone arc lengths are correlated with atmospheric CO<sub>2</sub> levels. The model spans much of the Phanerozoic as it links the 410-250 Ma Domeier and Torsvik (2014) and the 230-0 Ma Müller

et al. (2016) plate motion models. Using open-source and cross-platform plate reconstruction software GPlates (<http://gplates.org/download.html>)–(<http://gplates.org/download.html>)

20 and a new pyGPlates Python application programming interface (API) (<https://www.gplates.org/docs/pygplates/>), we measure the length of subduction zones at 1 Myr intervals since 410 Ma and track the length of subduction zones that interact with carbonate platforms (CIC subduction zones) from the

Kiessling et al. (2003) compilation, the length of all subduction zones that do not intersect carbonate platforms (non-CIC subduction zones), and total global subduction zone lengths. Using the pyGPlates  
25 workflow (Doss et al., 2016), global subduction zone boundaries were extracted from the Matthews et al. (2016) plate motion model, and subduction zone geometries were adjusted to remove any overlapping line segments that would overestimate arc lengths through time. The pyGPlates library enables access to

common GPlates functions using the Python programming language, a framework that facilitates model analysis and data processing. Using the pyGPlates workflow (Doss et al., 2016), global subduction zone boundaries were extracted from the Matthews et al. (2016) plate motion model in 1 million year time steps from 410 Ma to present day. Importantly, subduction zone geometries were adjusted to remove any overlapping line segments that would overestimate arc lengths through time.

## 2.4 Computing the intersections of carbonate platforms and subduction zones

We test whether continental subduction zones ~~volcanic arcs~~ interacting with carbonate platforms are different from non-intersecting ~~arcs~~ portions of subduction zones in their contribution to global atmospheric CO<sub>2</sub> concentrations, and hence we track the lengths of subduction zones that both do and do not intersect with carbonate platforms in the overriding platecontinental crust. Carbonate platform geometries were converted to polygons using *grdmask* from the development version of Generic Mapping Tools (GMT) (v.5.2.1; Wessel et al., 2015) which created a Boolean-style mask consisting of closed domains with a value of 1 where carbonate platforms existed and 0 elsewhere. We identified polygons proximal to subduction boundaries through time using the exported subduction zone geometries from the pyGPlates workflow. We compute the signed-distance function, positive toward the overriding plate, on the surface of the sphere for all subduction zones and computed where the carbonate platforms lie within +448 km of the trench. The *grdtrack* tool in GMT was used to create large tracks of ~450 km-long cross-profiles perpendicular to subduction boundaries at a uniform spacing of 10 km, with ‘whiskers’ pointing in the direction of subduction (Fig. 1a). The whiskers had five evenly-spaced nodes to detect intersections with carbonate platform polygons. We determined the ~450 km-long inclusion distance by determining average arc-trench distances using the present-day ‘Volcanoes of the World’ database maintained by the Smithsonian Institution’s Global Volcanism Program (Siebert and Simkin, 2014). From a sample size of 1023 volcanoes, average arc-trench distances are 287 km with a standard deviation of 161 km, which gives an upper estimate distance of 448 km. This captures ~84% of the location of all volcanic arcs and corresponds to an upper limit for interactions with volcanic arcs in our assumptions. The whiskers function as a buffer, allowing us to identify the lengths of subduction zone boundaries within ~450 km perpendicular radius of a carbonate platform polygon. Cross-profiles that overlap with carbonate platform



polygons demarcate areas where [continental arc-volcanoesubduction zones](#) interact with crustal carbonates (Fig. 1b). Due to the complexity and time-variability of subduction, we do not consider times during which flat slab subduction may have occurred, which would result in greater arc-trench distances and is beyond the scope of this study.

### 5 **3 Linking arc volcanism to palaeoclimate change**

Relationships between oscillations in two time-series can be examined using a wavelet analysis to elucidate the scales and time intervals where the proxy record and modelled data display correlated, periodic signals.

We performed wavelet analysis as a means of identifying localised variations of power between proxy records of CO<sub>2</sub> and modelled [carbonate-intersecting arc activityCIC subduction zone lengths](#) and in turn investigate the temporal evolution of these aperiodic signals. We are able to carry out this analysis as the geophysical data exhibit non-stationarity; dominant periodic signals vary in their frequency and amplitude through time. The continuous wavelet transform (CWT) is particularly useful for this task as it better characterises oscillatory behaviours of signals than discrete wavelet transforms. The CWT was applied to decompose arc lengths and proxy signals into time and frequency space simultaneously using functions (wavelets) that vary in width to discern both the high and low frequency features present (Lau and Weng, 1995; Supplement 3). To examine whether trends in atmospheric CO<sub>2</sub> and carbonate-intersecting arcs are connected in some way, the cross-wavelet transform (XWT) was carried out between the proxy-CO<sub>2</sub> data (Fig. S1) and each of the modelled data on carbonate-intersecting arc lengths (Supplement 4). The XWT reveals space-time regions where the two datasets coincidentally have high common power as well as calculating the phase relationships between signals, indicating where two series co-vary (Grinsted et al., 2004). Wavelet coherence (WTC) is computed in tandem with the XWT and determines if the time series are significantly interrelated in the frequency domain.

All wavelet analysis was carried out for each detrended and filtered time series using the Wavelet Coherence Toolbox™ for MATLAB® based on the statistical approach applied to geological and geophysical data by Torrence and Compo (1998) and Grinsted et al. (2004).

### 3.1 Data filtering

The modelled results and proxy-CO<sub>2</sub> time series were pre-processed for wavelet analysis by detrending and applying a low-pass filter using MATLAB®'s Signal Processing Toolbox™. The proxy-CO<sub>2</sub> time series is non-uniformly distributed with multiple data values at certain time steps. Prokoph and Bilali (2008) stress the importance of keeping a consistent time-scale across all time-series when examining causation between trends. Therefore, the data were first processed so that the median atmospheric CO<sub>2</sub> (ppm) value was taken at all time steps with multiple observations (Fig. S1). The data were then resampled with the MATLAB *resample* function to have 410 uniformly spaced data points across the 410 Myr timeframe. The function interpolates the time series linearly, and the series was found to be relatively insensitive to the interpolation method used. A moving average filter was applied using the MATLAB *filter* function with a window size of 7 [Myr](#) to remove high-frequency [noise signals that may represent noise or other short-term perturbations](#) (Fig. S2). In the time-frequency domain, our focus is on the power in the mid-to-high frequency spectrum and so the moving average filter was designed to remove periods less than 5 Myrs. As a result, the analysis does not capture any geologically-rapid (few Myrs) changes in CO<sub>2</sub> that may be driven by changes in plate tectonics and carbonate platform-arc interactions.

Rather than comparing estimates from the Accumulation Model with Phanerozoic atmospheric CO<sub>2</sub> models like COPSE (Bergman et al., 2004) or GEOCARBSULF (Bernier, 2006), results were compared to the proxy-CO<sub>2</sub> record compiled by Park and Royer (2011) because the unresolved uncertainties in model calculations may have rendered comparisons less meaningful than when comparing with proxy records. The proxy-CO<sub>2</sub> dataset presented by Park and Royer (2011) is an expanded version of the Royer (2006) collection, which originally incorporated data from 490 sources from the Phanerozoic (542 Ma to present) to present including palaeosols, foraminifera, stomatal indices,  $\delta^{11}\text{B}$  in marine carbonates and the  $\delta^{13}\text{C}$  of liverworts. The collection was chosen as it is the most up-to-date proxy-CO<sub>2</sub> data with the highest temporal resolution available.

## 4 Results

### 4.1 Continuous Wavelet Transform (CWT)

~~CIA-CIC subduction zone~~ lengths exhibit ephemeral mid- to long-wavelength periodicities that appear to dominate for prolonged time intervals, yet are completely absent ~~in other intervals during others~~. ~~A~~ The most significant periodic component in the 24-48 Myr band exists ~~from 300 to 300--350 Ma, returning 225-125 Ma and~~, however, the signal disappears in the following time period between 300 and 225 Ma (Fig. 2a). The 24-48 Myr periodic signal returns between 225 to 125 Ma, transitioning into the 48-60 Myr band between 150 and 100 Ma (Fig. 2a). ~~Between 100 and 50 Ma, significant power in the signal returns in the 14-48 Myr band.~~ In contrast, there are broad regions where signals of mid- to long-wavelength components remain strong in the ~~NCIA-non-CIC subduction zone~~ length data (Fig. 2b). Notably, the strongest significant signal components are in the 48-96 Myr band ~~in the 325-125 Ma time period~~ and the 24-32 Myr band ~~over a similar time period (325-125 Ma), in the 325-100 Ma time period,~~ demarcating a broad region of power where, conversely, there is distinctly no signal component in the ~~CIA-CIC subduction zone~~ length signal (Fig. 2a). At certain time periods the 10-18 Myr signal component in ~~non-CIC subduction zone~~ NCIA-lengths becomes significant, which is not identifiable in ~~CIA-CIC subduction zone~~ data.

Total global subduction zone lengths have ~~a number of several~~ clear and persistent signals through time, primarily in the 24-32 Myr, 48-64 Myr and 100-128 Myr waveband (Fig. ~~2d2c~~). ~~However,~~ ~~T~~he long-term, 100-128 Myr periodicity is not well localised in time as much of the result lies outside the COI.

Intermittent, sporadic regions of short- to mid-wavelength signal components appear in the proxy-CO<sub>2</sub> record, with the highest peaks within a confidence level of 95% occurring between 350 to 250 Ma (Fig. ~~2e2d~~). During this time period, a prominent peak of ~32 Myr cycles appears, transitioning into a broader 12-36 Myr band between 300 and 250 Ma (Fig. 2c). There is very little overlap in oscillatory behaviour between the subduction zone length results and the proxy-CO<sub>2</sub> record.

~~No other waveband in the proxy CO<sub>2</sub> record is characterised by significant spectral power within the COI.~~

|

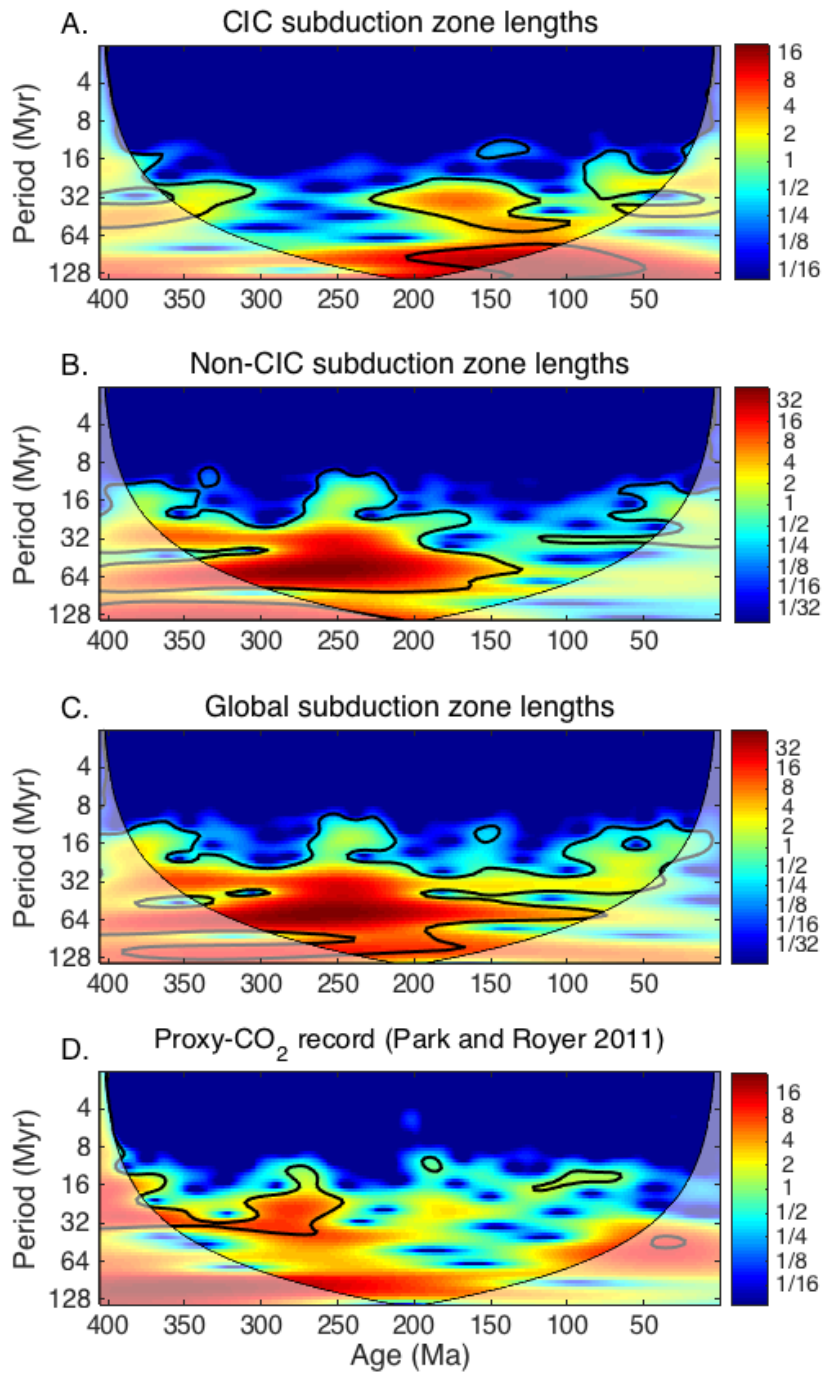


**Figure 2:** Continuous wavelet transforms (CWT) for (a) ~~CIA-CIC and (b) non-CIC- and (c) global subduction zone lengths;~~ (b) ~~NCIA lengths;~~ (c) ~~total global subduction zone lengths~~ and (d) the proxy-CO<sub>2</sub> data from Park and Royer (2011). Thick black contours designate the 5% significance level against a red noise background spectrum. The cone of influence (white translucent region) is where edge effects distort the spectrum. The colour bar indicates the wavelet power, with hotter colours corresponding to the maxima. Note the logarithmic scale of the Period (Myr) axis.

## 4.2 Cross-wavelet Transform (XWT) and wavelet coherence (WTC)

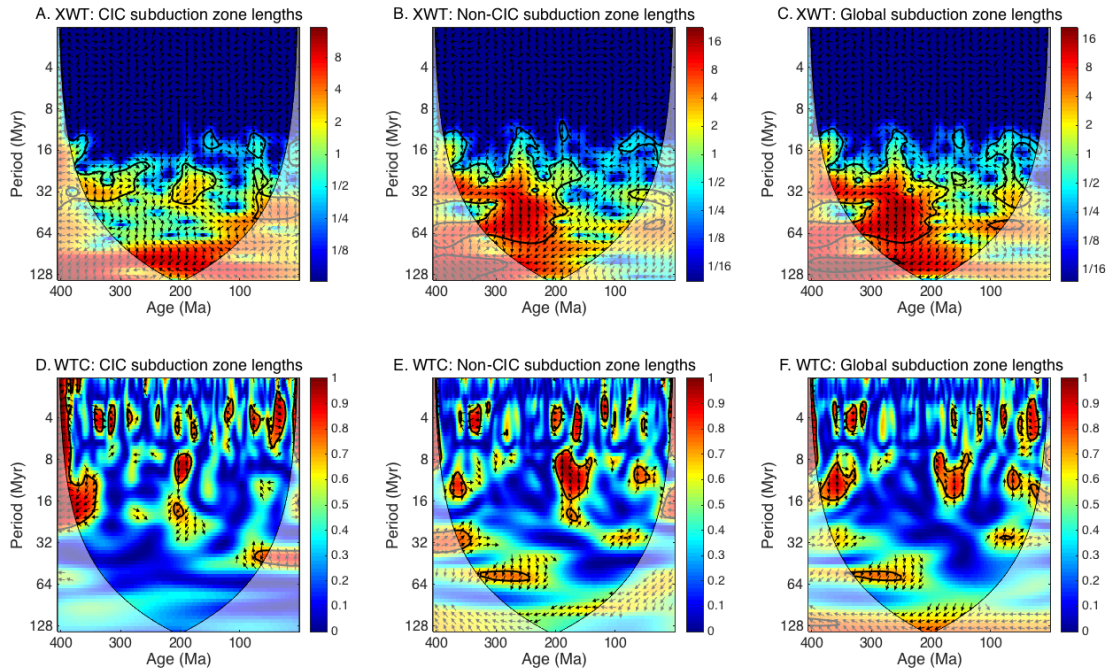
The periodic terms common in the ~~are~~ ~~subduction zone~~ length time series and the proxy-CO<sub>2</sub> record were investigated further using XWT and WTC (Fig. 3). Generally, the WTC analysis between subduction zone lengths and the proxy-CO<sub>2</sub> record do not highlight appreciable significant nor prolonged coherence through time.

While many Figure 3 shows the XWT comparing the proxy data and the carbonate intersecting are lengths data. Strong joint power at scales greater than 64 Myrs was detected between both the CIA lengths and NCIA lengths and the proxy CO<sub>2</sub> record, however, the result is never above the 95% confidence level (Fig. 3b).

Intervals of high joint power in the XWT spectra between CIA-CIC subduction zone lengths and proxy-CO<sub>2</sub> trends are exhibited, primarily in the 24-48 Myr waveband (Fig. 3a), only (410-280 Ma, 210-150 Ma and 75-0 Ma) are interspersed with intervals of low joint power (280-210 Ma and 150-80 Ma). In the ~32 Myr band during 360-280 Ma, peaks in CIA activity precede peaks in palaeo-atmospheric CO<sub>2</sub> by close to 90° and in the ~40 Myr band during 75-0 Ma, where the majority of the significant region lies outside the COI (Fig. 3a). In other words, during these intervals CIA activity leads atmospheric CO<sub>2</sub> levels by ~6-8 Myr. Only the interval from 75-0 Ma is confirmed by WTC as being coherent through time, although the majority of the significant region lies outside the COI and thus is not localised in time (Fig. 3d). In this interval, phase-locked arrows pointing north indicate that CIC subduction zone activity precedes peaks in palaeo-atmospheric CO<sub>2</sub> by close to 90° in the ~40 Myr waveband. The WTC confirms the significance of high-cross amplitudes in other regions as well (380-320 Ma and 200-180 Ma), however phase arrows show that CIC lengths lag CO<sub>2</sub> peaks by ~approximately -60° (2-4 Myrs), indicating anti-correlated behaviour (Fig. 3d). In the 210-150 Ma time interval, CO<sub>2</sub> peaks exhibit a ~45-90° lead (~5 Myr) over CIA activity to the anti phase in the 20-40 Myr band (Fig. 3a). Considering the non-



uniqueness problem outlined by Grinsted et al. (2004), the region of 90° phase difference may also be interpreted as a ~5 Myr in phase lag of CO<sub>2</sub> after CIA peaks. The lack of significant coherence in this region suggests coincidence rather than causation.



5

**Figure 3:** The cross-wavelet transforms (XWT) (top) and wavelet coherence (WTC) (bottom) for (a,d) CIA-CIC lengths, (b,e) NCIA lengths:non-CIC and (c,f) total global subduction zone lengths respectively and the proxy-CO<sub>2</sub> record (Park and Royer 2011). Thick black contours designate the 5% significance level against a red noise spectrum. The white translucent region designates the cone of influence (COI). The colour bar indicates the magnitude of cross-spectral power for the XWT, and for the WTC it represents the significance level of the Monte-Carlo test. The arrows indicate the phase relationship of the two time series in time-frequency space, where east-pointing arrows indicate in-phase behaviour, west-pointing arrows indicate anti-phase behaviour, north-pointing arrows indicate that the peaks in are or subduction zone activity-lengths leads the CO<sub>2</sub> peaks and south-pointing arrows indicating that CO<sub>2</sub> peaks lead peaks in are or subduction zone activitysubduction zone lengths.

10

15

The WTC between CIA lengths and the proxy CO<sub>2</sub> record does not show appreciable nor prolonged coherence through time (Fig. 3d). However, at distinct intervals the WTC confirms the significance of three regions of high cross amplitudes: the 14-24 Myr periodicity between 380-360 Ma; the 18-24 Myr periodicity between ~200-180 Myr; and the 40-48 Myr periodicity from 75-0 Ma (although much of the significant region lies outside the COI and thus is not localised in time). Phase arrows for periodicities

prevalent during 380–360 Ma and 200–180 Ma indicate that CIA length peaks are anti-correlated with CO<sub>2</sub> peaks and lag by ~60° (2–4 Myrs) whereas from 75–0 Ma, locked phase arrows in the 20–40 Myr band indicate arc length peaks lead CO<sub>2</sub> by approximately 90° (10 Myrs) (Fig. 3d). Large regions in the 24–40 Myr band of high joint power (i.e. for 410–280 Ma and 210–150 Ma) were not confirmed by wavelet coherence (Figs. 3a, 3d).

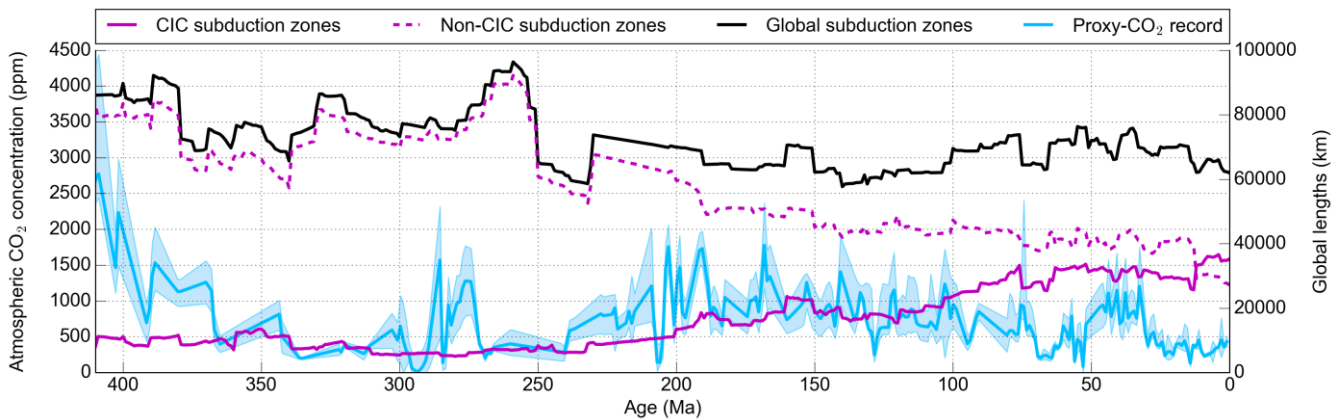
NCIA-P peaks in non-CIC subduction zone lengths also shares high joint power with proxy-CO<sub>2</sub> peaks at similar intervals to CIA peaks-CIC subduction zones in the 20–48 Myr band, but in contrast shows very high joint power between 275–200 Ma where CIC subduction zone CIA peaks do not (Fig. 3b). In the longer-wavelength band (40–80 Myr) between 300–200 Ma, high joint power exists between NCIA-non-CIC subduction zone lengths and proxy-CO<sub>2</sub> peaks; a trend not exhibited in CIA-CIC subduction zone activity (Figs. 3b, 3a). While this region timeframe is coherent, it exhibits anti-correlated phase behaviour (Fig. 3e).

The phase relationship shows the opposite of climate forcing behaviour, where NCIA peaks lag 8–20 Myrs behind palaeo-atmospheric CO<sub>2</sub> peaks.

Only a few significant areas of the XWT between NCIA-non-CIC subduction zones and proxy-CO<sub>2</sub> data is confirmed by wavelet coherence above the 95% confidence level. Some of these areas are common for between proxy CO<sub>2</sub> and both CIA and NCIA-CIC and non-CIC subduction zone lengths (, specifically at 375–360–340–350 Ma and ~201–90–180–75 Ma) (Figs. 3d, 3e). Of these intervals, phase arrows in the 200–180 Ma interval in the 10–24 Myr waveband show synchronised phase behaviour indicated by north-pointing facing arrows (Fig. 3e). In the 10–15–16 Myr waveband between 360–340–375–350 Ma, anti-phase, negatively-correlated behaviour exists where palaeo-atmospheric CO<sub>2</sub> peaks lead NCIA-non-CIC subduction zone lengths by approximately 90° (3–4 Myrs) (Fig. 3e). Considering the non-uniqueness problem of phase analysis, this could be interpreted as a positively correlated signal with arc activity leading palaeo-atmospheric CO<sub>2</sub>. This trend is also exhibited between CO<sub>2</sub> peaks and CIA-CIC subduction zone lengths during a similar time interval (Fig. 3d).

Between 400 ~~360 and 340~~ and 350 Ma, significant coherence confirms cross-spectral power and closely in phase behaviour in the 30-32 Myr waveband of NCIA lengths, yet most of the significant region lies outside the COI (Figs. 3b, 3d).

Phase arrows in the ~64 Myr band between 310 and 250 Ma suggest palaeo-atmospheric CO<sub>2</sub> peaks led NCIA peaks by approximately 10 Myrs, the opposite of climate forcing behaviour. The XWT and WTC for proxy-CO<sub>2</sub> correlations with total subduction zone lengths exhibit ~~similar a very similar spectrum to results for to NCIA-non-CIC subduction zone lengths~~ (Figs. 3e, 3f), ~~particularly regarding phase-locked behaviour in the 10-16 Myr waveband region~~ range between 375-350 Ma and 200-180 Ma (Figs. 3e, 3f). ~~One exception is that coherence in the 30-32 Myr waveband becomes dominant between 90-70 Ma, where a correlation that was not above the 5% significance level when examining NCIA non-CIC subduction zone lengths.~~ Phase relationships in this interval indicate that in-phase CO<sub>2</sub> peaks are leading by ~60° (~5 Myrs) (Fig. 3f). ~~In-phase, coherent oscillatory behaviour at this time is also present between CO<sub>2</sub> peaks and CIC subduction zone lengths (Fig. 3d).~~



15

**Figure 4:** Total global lengths of subduction zones (black) (as a surrogate measure for volcanic arc lengths) compared with arc-lengths of all subduction zones that intersect with buried crustal carbonate platforms (magenta, solid) and arc-those lengths that do not intersect crustal carbonate platforms (magenta, dashed). The proxy-CO<sub>2</sub> record (blue line) from Park and Royer (2011) with upper and lower bounds (blue envelope) are displayed for comparison.

### 4.3 Comparing carbonate-intersecting arc length and palaeo-CO<sub>2</sub> trends

Coherence analysis suggests that CIA-CIC subduction zone lengths and palaeo-atmospheric CO<sub>2</sub> peaks may not be well correlated prior to 100 Ma. Indeed, CIC subduction zone lengths make up a small proportion of global subduction zones prior to 200 Ma, beginning at 7940 km at 410 Ma and increasing to over 15 000 km only after 200 Ma (Fig. 4). However, during some time windows, periodic behaviour may be correlated. These three areas of significance highlighted by the XWT and WTC analysis are between 380-~~350~~-320 Ma, 210-1890 Ma and 75-50 Ma (Fig. 3).

Between 380- and 3250 Ma, coherence analysis highlights possible in-phase 30-32 Myr linked periodic behaviour between-for both global and non-CIC subduction zone lengths and NCIA lengths and with CO<sub>2</sub> peaks, which is validated by trend data ~~despite much of the significant region lies outside the COI~~ (Fig. 3d). Over the period 380-340, D decreasing non-CIC and global total subduction zone and NCIA lengths mirror the CO<sub>2</sub> record trend as lengths drop from ~~~92-77~~ 000 km to ~~~69-54~~ 000 km and ~~~83-88~~ 000 km to ~~~57-66~~ 000 km respectively (Fig. 4), ~~yet the signal was coherent at the 95% significance level for NCIA lengths (Figs. 3e, 3f).~~ In contrast, wavelet analysis found ~~the opposite of climate forcing behaviour for CIA lengths over this interval where anti-correlated behaviour between CIC subduction zone lengths and the CO<sub>2</sub> peaks led CIA lengths record~~ (Fig. ~~3e3d~~), and in line with the analysis, CIA-CIC subduction zone lengths remain relatively low (~~7 0003-000-120~~ 000 km) over this period (Fig. 4). It is evident that the magnitude of change in CIA-CIC subduction zone lengths cannot explain the precipitous drop in palaeo-atmospheric CO<sub>2</sub> (2 750 ppm to 200 ppm) taking place from ~410 Ma to ~340 Ma (Fig. 4).

~~Non-unique interpretations of phase behaviour in the WTC are non-conclusive regarding whether total subduction zones, CIA or NCIA activity or CO<sub>2</sub> peaks are leading d~~ During the 210-190 Ma interval. ~~It appears in the XWT and WTC that CIA activity lags palaeo-atmospheric CO<sub>2</sub> peaks, whereas NCIA activity and total subduction length peaks lead palaeo-atmospheric CO<sub>2</sub> peaks (Figs. 3e, 3f, w).~~ We observe a rapid reduction in NCIA-non-CIC subduction zone lengths (~~~6135-000~~ to 50000-48 000 km) and global subduction zones (~~~ 71 000~~ to 65 000 km) simultaneously with a relatively dramatic increase CIA-CIC subduction zone lengths, ~~which almost double~~ (~~~7400-10 37000~~ to ~16300-17 000 km), between

~~210-190 Ma~~ (Fig. 4). ~~However, as only Short-wavelength small-scale~~ periodic behaviour (~10 Myrs) exists for palaeo-CO<sub>2</sub> but ~~and mid- to long-wavelength behaviour for CIC and non-CIC subduction zone lengths, which implies not for CIA or NCIA lengths during this period point to~~ a scale mismatch ~~evidenced by CWT analyses in the CWT results~~ (Fig. 2). Hence, neither ~~CIA, NCIA, CIC, non-CIC nor~~ global subduction zone lengths can adequately explain large-amplitude (~45 ~~to~~ 1 800 ppm), high-frequency (~10 Myr) fluctuations in palaeo-atmospheric CO<sub>2</sub> levels over the 210-190 Ma ~~period~~ timeframe (Fig. 4).

Between 75-0 Ma, XWT and WTC analysis highlighted a significant domain of high coherence between ~~CIA-CIC subduction zone~~ length data and the proxy-CO<sub>2</sub> record in the 40-48 Myr waveband with an arc-leading relationship of ~10 Myrs (Figs. ~~3a, 3e, 3d, 3d~~). Over the same time interval, an area of high coherence with arc-leading relationships occurs in the ~32 Myr waveband between global subduction zone lengths and the proxy-CO<sub>2</sub> record (Figs. ~~3ce, 3f~~). This result is reflected in trend data, where ~~CIA both CIC~~ and global subduction zone lengths reach a local maximum at ~75 Ma (~~~32-26~~ 000 km and ~74 000 km respectively), drop sharply for a period of ~10 Myrs before recovering between 63- ~~and~~ 50 Ma (on average ~32 000 and ~72 000 km in length, respectively) (Fig. 4). The proxy-CO<sub>2</sub> data mirror this decline-and-recovery trend, as palaeo-atmospheric CO<sub>2</sub> levels decline substantially between 75- ~~and~~ 70 Ma (~1200 ppm to ~250 ppm) and recover after 60 Ma (~700 ppm) (Fig. 4). ~~Non-CIC-CO<sub>2</sub> XWT NCIA-CO<sub>2</sub>-XWT~~ results highlight significant joint power during the same interval, but it was not confirmed as coherent behaviour by the WTC (Fig. 3b, 3d). In accordance, ~~NCIA-non-CIC subduction zone~~ lengths do not sustain the same linked behaviour as CIC and global subduction zone ~~CIA and global subduction~~ lengths over this interval.

## 5 Discussion

~~From 250 Ma, the Accumulation Model~~ accumulated carbonate platforms consistently ~~made up~~ intersect ~ 70% of total global subduction zone lengths (Fig. 4). Given this ~~cumulative~~ significant effect, ~~The Accumulation Model was constructed in a way that resulted in increased subduction zone interactions with carbonate platforms in the overriding plate through time. Indeed from 150 Ma onward, CIA lengths consistently made up ~70% of total global subduction zone lengths (Fig. 4). Given this cumulative effect,~~

we would expect that the growing reservoir of carbonate platforms would result in linked, periodic behaviour in the more recent past compared to 400-250 Ma if [the length of CIAs-CIC subduction zones had a dominant climate-forcing effect. CIC subduction zone lengths and the proxy-CO<sub>2</sub> record are largely independent with no strong leader relationship that is consistent through time, with the exception of the most recent ~75 Myr.](#) Ultimately, our study does not support the hypothesis that carbonate-intersecting arcs ~~have contributed~~[have had a sustained and dominant influence on-substantially to](#) atmospheric CO<sub>2</sub> levels over the past 410 Myrs. [Instead, carbonate-intersecting subduction-derived magmatism is likely to have episodic control on atmospheric CO<sub>2</sub>, perhaps related to the inception or abandonment of major regional continental subduction zones.](#) However, potential issues with the large uncertainties in the proxy record, complexities in reconstructing pre-Pangea subduction zones and carbonate platforms, as well as the requirement to filter the time series may influence this result.

[At present day, our estimates of CIC and global subduction zone lengths reach approximately 35 000 km and 62 000 km respectively. Recent calculations of global continental arc lengths by Cao et al. \(2017\) are approximately 15 000 km, which are more than half of our calculations for CIC subduction zone lengths only. Cao et al. \(2017\) are ~~only~~focussed on measuring the extent of continental volcanic arcs, whereas our investigation encompasses ~~all~~the total segment lengths of all subduction zones, ~~and~~including those that intersect carbonate platforms. ~~We have attempted to encompass~~capture the ~~contribution~~all possible effects](#)Therefore, our analysis tends to capture a broader range of CO<sub>2</sub> degassing mechanisms along subduction zones, ~~o~~including diffuse outgassing from fore-arcs, back-arcs and volcanic arcs along faults, fractures and fissures, in addition to arc volcanoes. This is because melt is ~~inevitable~~ubiquitous ~~everywhere~~along subduction zones, and there is very little carbon storage along arcs (Keleman and Manning, 2015). For this reason, our ~~measurements~~approach differs from ~~are~~that ~~irreconcilable~~with those ~~by~~of Cao et al. (2017), as we are attempting to ~~represent~~capture ~~all~~additional mechanisms of CO<sub>2</sub> escape along continental subduction zones, as opposed to only those directly associated with volcanic arcs, and our ~~and~~estimates ~~represent~~may be regarded as an upper bound ~~estimate~~on total CO<sub>2</sub> emissions at subduction zones.



~~CIA lengths and the proxy CO<sub>2</sub> record are largely independent with no strong leader relationship that is consistent through time, with the exception of the most recent ~75 Myrs.~~

Wavelet analysis highlights many intervals of significant and high joint power in all XWT spectra, yet they were not coherent and thus could not be distinguished from coincidence, such as the region of high power in ~10-64 Myr wavebands from 300-200 Ma for ~~non-CIC and~~ global subduction zone lengths ~~and NCIA lengths~~ (Figs. 3b, 3c). In some intervals, wavelet analysis highlights the opposite of climate-forcing behaviour between ~~CIA-CIC subduction zone~~ lengths and palaeo-atmospheric CO<sub>2</sub> levels (i.e. where CO<sub>2</sub> peaks precede ~~are-subduction zone~~ lengths), such as between 210 and 190 Ma (Fig. 3a). Similarly, a long-lived coherent ~64 Myr signal in both the ~~non-CIC subduction zone NCIA~~ lengths and global subduction zone lengths was found to be a significantly coherent signal at the 95% level (Figs. 3e, 3f), yet the CO<sub>2</sub> peak occurred ~16 Myrs prior to ~~non-CIC NCIA~~ and global subduction length peaks and the result was not found to be meaningful in the context of climate-forcing behaviour (Fig. 4).

A 30-32 Myr periodicity in the ~~NCIA-non-CIC subduction zone~~ length signal in the 375-350 Ma interval may be interpreted as being linked to a concomitant decline in palaeo-atmospheric CO<sub>2</sub>, a relationship which was similar in the global subduction zone lengths signal yet was insignificant at the 95% level. Both palaeobotanical and modelling investigations suggest that the rise of vascular land plants (Algeo et al., 1995) and heightened chemical weathering (Bernier and Kothavala, 2001) were the dominant forces controlling the large reduction in atmospheric CO<sub>2</sub> during the Late Devonian, however, this result does not preclude the notion that waning ~~CIA-CIC subduction zone~~ lengths may have partially contributed to the cooler background climate. Our results suggest that ~~subduction zone are~~ lengths have not consistently modulated the CO<sub>2</sub>-forced transitions between warmer and cooler climates throughout the Phanerozoic. However similar trends in ~~CIC subduction zone CIA~~ lengths and global subduction zone lengths between 75-50 Ma suggest that the Late Cretaceous to ~~Early-early~~ Palaeogene warm climate may be a phenomenon forced by global subduction zone lengths rather than ~~CIC carbonate intersecting-subduction zone are~~ lengths alone.

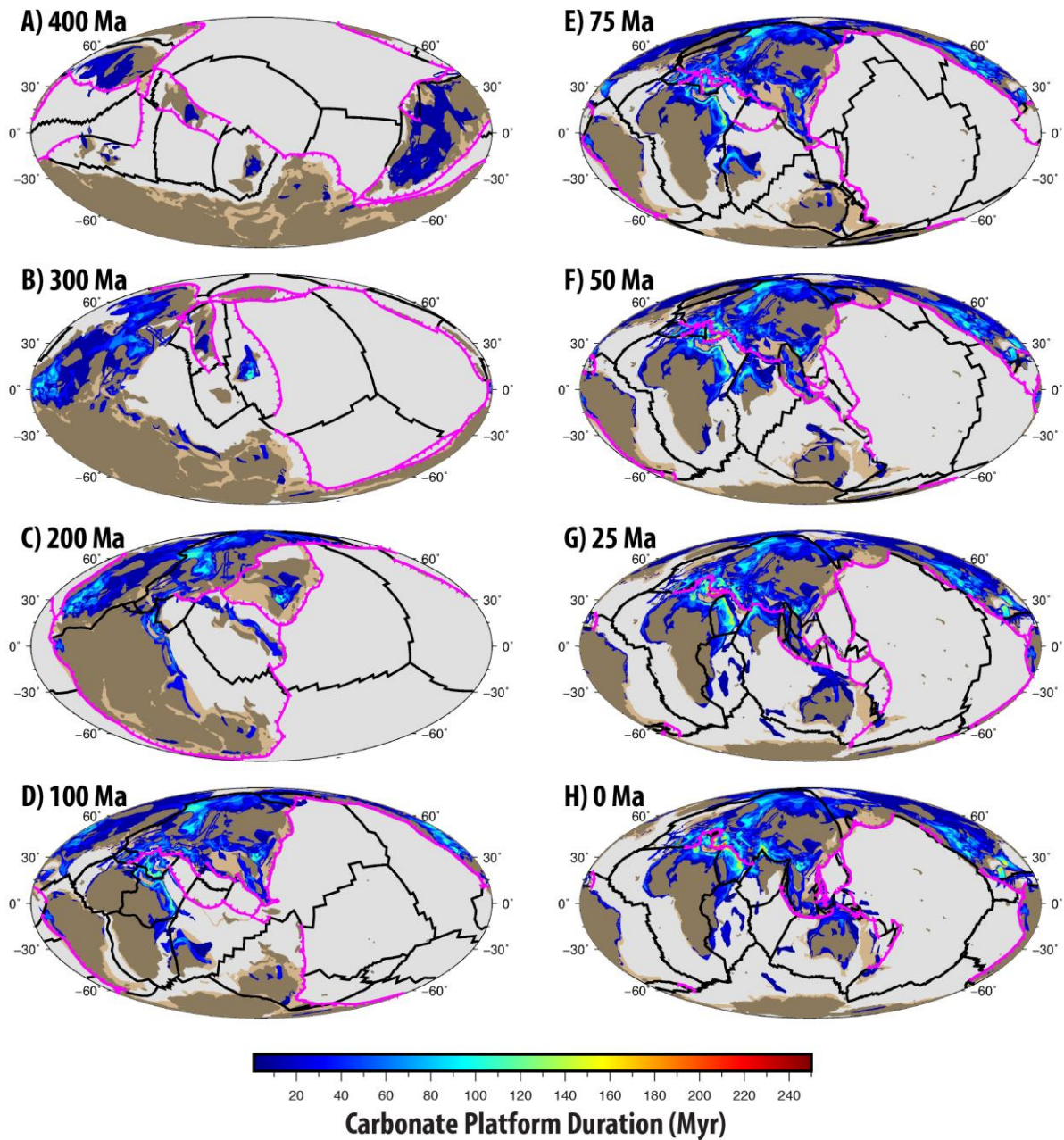


**Figure 5:** Plate reconstructions with plate boundaries (black), subduction zones (purple) and distributions of carbonate platforms. Carbonate platforms are distributed according to the Accumulation Model at [key intervals from 400 Ma to present day, 0, 75 and 80 Ma](#). Colour bar corresponds to the duration of time that the carbonate platforms were actively developing for in the crust.

## 5.1 Implications for Late Cretaceous to Early Palaeogene Climate

Only during the most recent 75 Myrs is it plausible that [CIC subduction zone CIA](#)-lengths influenced atmospheric CO<sub>2</sub>; [based on our analysis](#), yet there are two factors that prevent us from viewing these correlations as causative. Firstly, while the ~32 Myr cyclicity is coherent and significant at the 5% level, it is not time-localised between 60-0 Ma as the result lies outside the COI. Secondly, [CIC subduction zone CIA](#)-length trends passively mirror total global subduction zone lengths during this time, suggesting that it is not specifically the CO<sub>2</sub> liberated at [CIC subduction zones CIAs](#) that drove atmospheric CO<sub>2</sub> peaks, but net global ~~volcanic~~ CO<sub>2</sub> emissions [along subduction zones](#).

However, the period between 75-50 Ma seems to be distinct from other times as a significant coherency occurs. The changing distribution of [CIC subduction zone CIA](#)-lengths and subduction zones between 75 and 50 Ma may have contributed to the well-studied greenhouse climate 51-53 Ma, known as the Early Eocene climatic optimum (EECO), where temperatures were about  $14 \pm 3^\circ\text{C}$  warmer than the pre-industrial period (Caballero and Huber, 2013). While climate interactions and feedbacks leading to the greenhouse state remain uncertain, climate sensitivity to CO<sub>2</sub> forcing is likely (Anagnostou et al., 2016).

According to the Accumulation model, the dramatic change that characterised the reduction in [CIC subduction zone CIA](#)-lengths ~75 Ma included the termination of a ~3 000-km-long section of a north-dipping intra-oceanic subduction zone in the Northern Tethys ocean, corresponding to the Trans-Tethyan Subduction System (Jagoutz et al., 2016), and the cessation of subduction along the Sundaland margin (McCourt et al., 1996; Zahirovic et al., 2016) (Figs. [5de](#), [5ed](#)). The intra-oceanic subduction in the Neo-Tethys in our model would not be classified as a carbonate-intersecting ~~arc~~ [subduction zone](#) due to the overriding plate (in this case largely oceanic lithosphere) lacking extensive carbonate platforms. In any case, this intra-oceanic subduction zone in the Accumulation Model corresponds to the emplacement of the peri-Arabian ophiolite belt along the Afro-Arabian continental margin between 80-70 Ma rather than an Andean-style arc, the erosion of which has been posited as a cause of global cooling following the EECO (Jagoutz et al., 2016) (Figs. [5de](#), [5ed](#)). We can therefore rule out ~~arc~~ [subduction-zone](#)-related volcanism in this region as a contributor to high CO<sub>2</sub> levels given that the shut-down of this arc is not associated with the cessation of Andean-style subduction.

The termination of arc volcanism particularly along the Sundaland margin, where a large area of carbonate platforms are buried, contributed ~3 000 km to the global reduction in [CIC subduction zone CIA](#)-lengths by ~7 000 km between 75-65 Ma (Figs. [5b5e](#), [5fe](#)). The resumption of subduction along the Sunda-Java trench at 65 Ma in the model as well as the emplacement of a set of carbonate platforms in the lower latitudes at 63 Ma explain the modelled results of an increase in [CIC subduction zone CIA](#)-lengths at 63 Ma which persist past 50 Ma (Fig. [5b5f](#)). The EECO occurred approximately 10 Myr later, supporting the 10 Myr lag in peaks of a ~40 Myr periodicity found by the [CIC CIA](#)-proxy-CO<sub>2</sub> XWT and WTC (Fig. 3a). Our analysis shows a concomitant increase in [non-CIC subduction zone NCIA](#)-lengths (Fig. 4), but the periodic behaviour was not found to be significantly coherent and so coincidental peaks cannot be ruled out. Modern volcanic CO<sub>2</sub> output from arcs in Indonesia, Papua New Guinea, parts of the Andes and Italian Magmatic Province are strongly influenced by carbonate assimilation (Mason et al., 2017) and volcanoes in those regions currently contribute significantly to global atmospheric CO<sub>2</sub> flux (Carter and Dasgupta, 2015). Assuming a similar subduction style, this result gives plausibility to the idea that volcanic activity along the Sunda-Java trench during the Cretaceous was also significantly contributing to global CO<sub>2</sub> output.

Previous studies have suggested that global arc CO<sub>2</sub> contributed to the baseline warm climate of the Late Cretaceous and late Palaeogene, due to the greater size of carbonate reservoirs in continents and the increased continental arc lengths (Lee et al., 2013; Carter and Dasgupta, 2015; McKenzie et al., 2016; Cao et al., 2017). Our results agree well with the hypothesis, as a relative increase in [CIC subduction zone CIA](#)-lengths has been linked to a peak in atmospheric CO<sub>2</sub> from 75-50 Ma, contributing to enhanced CO<sub>2</sub> degassing. However, it cannot be determined from this study whether the increase in global [arc-subduction zone](#) lengths is more important than the relative increase in [the lengths that intersect carbonate platforms CIA-lengths](#).

## 5.2 Limitations of wavelet analysis

Wavelet analysis is inherently sensitive to the shape of signals, and as such, adjustment of filtering and processing techniques introduces variations in the results. [Firstly, the proxy-CO<sub>2</sub> signal applied here is a mean signal between reported standard deviations on proxy data \(Park and Royer, 2011\). While the](#)

uncertainties appear to be time-localised, the uncertainty in CO<sub>2</sub> concentrations in the proxy record could not be captured by our method of extracting only one signal. Moreover, the choice of interpolation method of the proxy-CO<sub>2</sub> record may subdue actual oscillations in the signal, affecting phase relationships and confidence intervals. Similarly, a size-7 moving average window filter was chosen to remove high-frequency noise, yet it may have moved trends forward in time, which ultimately changes whether peaks overlap or not and adds uncertainty to results. Peaks in the XWT were robust in that they were found to appear in XWT plots regardless of the intensity of smoothing, yet the significance contours differed strongly due to smoothing. For instance, with a longer low-bandpass filter, small-scale oscillations <5 Myrs were removed, reducing areas of significant power in the shorter wavebands. Similarly, when experimenting with a high-bandpass filter, significant regions were directed away from the longer periodicities of >64 Myrs to shorter periodicities. The low-bandpass filter was chosen to remove the noise for smaller periodicities where fluctuations were less likely to represent trends and more likely to represent artefacts of interpolation, yet this measure erases the fidelity of short-term oscillations in the time series. Hence detail on the <10 Myr scale is not adequately represented, and thus our study was unable to evaluate short-term relationships.

Our analysis technique cannot quantify the error that propagates from uncertainty in the proxy-CO<sub>2</sub> record and ~~volcanic arc length~~ subduction zone length signal through to the correlation uncertainty. Interpolation and filtering of the proxy-CO<sub>2</sub> record necessarily cannot account for the uncertainty displayed by the envelope as only one signal can be extracted. Similarly, the Matthews et al. (2016) tectonic plate model represents one interpretation of geological data which becomes sparse for deeper geological time, especially earlier than for pre-Pangea times (before ~250-200-220 Ma). The nature of using a tectonic framework means only one subduction zone ~~arc~~-length signal can be extracted from the model, which does not lend well to estimations of error. In this way, the selection and comparison of two signals with large uncertainty are not sufficient in eliciting well-constrained periodic behaviour and true correlations. XWT analysis describes areas with high power which can be misleading when the XWT spectrum is not normalised. For instance, areas of high joint power were found where relatively flat peaks in the CIC subduction zone ~~CIA~~-length data occurred simply because of the large amplitude of peaks in the proxy-CO<sub>2</sub> data. The vast differences in magnitude do not necessarily constitute a causative relationship. WTC



analysis does not present this problem because the spectrum is normalised, and hence periodicities with strong power were not necessarily found to be coherent (Maraun and Kurths, 2004). The combination of both measures somewhat circumvents the problem of misleading peaks in the XWT, but not all. Given that wavelet analysis is very sensitive to magnitude and timing of peaks, the fact that the uncertainty in our modelled estimates of [subduction zone are-lengths](#) are not well-constrained introduces variability in correlative relationships.

Wavelet analysis, like other signal processing techniques, is limited by the length of the time series data investigated. Periods of greater than half the time series length cannot be examined using this method (Winder, 2002). Therefore, very-long oscillations on the scale of 250 Myr or more could not be derived from our data. One reason for examining patterns on 250 Ma periods is due to the very-long-term nature of supercontinent cycles. The accretion of supercontinents such as Pangea and Rodinia are associated with shortened continental [subduction zone are-lengths](#), whilst continental break-up and dispersal initiates subduction on the edges of continents, and thus increases continental [subduction zone are-lengths](#) (Donnadieu et al., 2004; [Lenardic et al. 2011](#); Lee et al., 2016). ~~These~~ ~~Not only do~~ changing modes of supercontinent break-up or accretion have the potential to influence climate, ~~the opposite causal effect may occur where changes in the long-term climate state can feed back into the coupled system and initiated changes in the tectonic regime (Lenardic et al., 2016)~~. Given that supercontinent cycles exceed 200 Myr in length and exert a large effect on the length of continental arcs (Lee et al., 2013), applying this analysis to plate reconstructions that capture multiple supercontinent cycles (e.g. Merdith et al., 2017) to investigate whether such long-term linkages exist between atmospheric CO<sub>2</sub> and [global subduction zone emissions](#) ~~global are volcanism~~.

### 5.3 Limitations of model assumptions

The extent to which our models are representative of ~~volcanic are~~ [subduction zone](#) CO<sub>2</sub> emissions is limited by some issues with the subduction zone quantification approach. The subduction zone modelling attempted to approximate ~~relative magmatic~~ [atmospheric CO<sub>2</sub> flux at subduction zones](#) without directly measuring it by assuming a constant CO<sub>2</sub> flux and a unit-correspondence of [subduction zone are-lengths](#) to volcanoes, [vents or fissures](#). Both assumptions are problematic. There are several dynamic factors that

govern ~~subduction-zone-are~~ CO<sub>2</sub> flux such as convergence rates (van der Meer et al., 2014), the composition and volume of subducted sediments (Rea and Ruff, 1996), convergence obliquity (Kerrick and Connolly, 2001), slab volume flux (Fischer, 2008), the relative contribution of metamorphic decarbonation in the crust and in the mantle wedge (Keleman and Manning, 2015) and the efficiency of decarbonation (Johnston et al., 2011). The model does not account for these factors and assumes that the parameters of CO<sub>2</sub> flux have remained constant in time. In addition, the number of volcanoes or vents per unit length of subduction zones is neither constant through time nor correlated, at least for the circum-Pacific arc and Central American arc (Kerrick, 2001). Furthermore, the Accumulation Model has no way to account for carbonate platform thicknesses, and thus cannot account for the realistic depletion of crustal carbonate reservoirs through time. The inability of the model to incorporate the complexity of depleting carbonate platforms may lead to sampling bias during continental collisions. This highlights an area of future improvement, including the utilisation of subduction zone geodynamic-geochemical modelling (e.g. Gonzales et al., 2016) by tracking different CO<sub>2</sub> reservoirs in a geodynamic context.-

Furthermore, uncertainty cannot be measured using our GPlates modelling approach. Uncertainty propagates ~~back~~ through the plate motion model ~~through~~ over deeper reaches of geological time, such that it is impossible to quantify uncertainty of all possible configurations of subduction zones, especially in the pre-Pangea timeframe. Moreover, there is a much greater uncertainty in the dynamic mechanisms of carbon cyclinge and geochemical processes at along subduction zones, and quantification of all geochemical decarbonation reactions is still in infancy (Gonzales et al., 2016). For these reasons, formal uncertainties ~~is assumed and qualified in this end-member scenario, but cannot yet be directly quantified for models of subduction zone carbon cycling.~~

Taking all limitations into consideration, the Accumulation Model still provides a first-order approximation of changing ~~subduction zone are~~ lengths through time and the interaction with (buried) carbonate platforms as a surrogate measurean indicator for of CO<sub>2</sub> degassing, especially for the ~~early Phanerozoic which had not previously been modelled at a 1 Myr resolution~~ Late Cretaceous and early Paleogene.



## 6 Conclusions

Wavelet analysis is a useful tool in elucidating coherent, phase-related periodicities between the CO<sub>2</sub> record and various climate forcing factors. Our analysis has revealed that [CIC subduction zone CIA](#) activity is largely independent to the proxy-CO<sub>2</sub> record over the past 410 Myr except for the period 75-50 Ma. The [CIC subduction zone CIA](#)-lengths that we derived from an Accumulation model of carbonate platform evolution do not find reasonable and persistent periodicities that explain atmospheric CO<sub>2</sub> flux, however there may be some causal relationships in the Late Cretaceous to [Early-early](#) Palaeogene that are supported by previous modelling efforts.

This analysis lends partial support to the idea that, at certain times, carbonate-intersecting [are-subduction zone](#) activity is more important than non-carbonate intersecting activity in driving atmospheric CO<sub>2</sub>, yet the climate system is vastly complex and the result could mean that other processes have dominated climate feedback mechanisms through time, such as the proliferation of terrestrial plant life (Algeo et al., 1995), silicate weathering (Kent and Muttoni, 2008) and the emplacement of large igneous provinces (Belcher and Mander, 2012).

Generally, an absence of constraints on carbon-climate interactions in deep-time makes it difficult to test hypotheses about greenhouse and icehouse climate states. Clearly, more [accurate-robust](#) reconstructions of climate-forcing processes are needed to improve our understanding of the deep carbon system. It is suggested that further investigations be carried out at specific time intervals to eliminate the uncertainty around the time periods within the COI at the end of the data series (between 410-350 Ma and 50-0 Ma).

With adjustments to the parameters and assumptions governing the carbonate platform evolution models, the data can be used as input into fully-coupled planetary-scale climate [and carbon cycle box](#) models. This would provide the most comprehensive and self-consistent approach to understand the contribution of [emissions at global are volcanism subduction zones](#) to the deep carbon cycle.

## Code and data availability

The subduction zone toolkit by Doss et al. (2016) was developed as a product of this research and has been made publicly available for use with open-source plate reconstruction software, GPlates. The toolkit includes all proxy CO<sub>2</sub> data, pyGPlates and bash scripts as well as the Matthews et al. (2016) plate model.

- 5 Both the Signal Processing Toolbox™ and Wavelet Coherence Toolbox™ for MATLAB® were used in analysis and the production of figures. The Wavelet Coherence Toolbox™ can be found at <http://noc.ac.uk/marine-data-products/cross-wavelet-wavelet-coherence-toolbox-matlab>, while the Signal Processing Toolbox™ can be found at <http://au.mathworks.com/help/signal/index.html>.

- 10 Doss, S., Zahirovic, S., Müller, D. and Pall, J: DCO Modelling of Deep Time Atmospheric Carbon Flux from Subduction One Interactions: Plate Models & Minor Edits, Zenodo, <http://dx.doi.org/10.5281/zenodo.154001>~~http://dx.doi.org/10.5281/zenodo.154001~~, 2016.

## Author Contribution

Sebastiano Doss and Jodie Pall developed the Subduction Zone toolkit together and carried out modelling experiments under the supervision of Dietmar Müller and Sabin Zahirovic. Figures were prepared by Jodie Pall and Sebastiano Doss, and the toolkit repository was prepared by Sebastiano Doss. Jodie Pall  
5 conducted wavelet analysis with assistance from Rakib Hassan. Jodie Pall also prepared the manuscript with contributions from all co-authors.

## Competing interests

The authors declare that they have no conflict of interest.

## Acknowledgements

10 The authors acknowledge and thank the [Alfred P Sloan Foundation and the](#) Deep Carbon Observatory (DCO) for funding this ~~deep carbon modelling and visualisation effort~~[research](#). We would also like to thank members of the EarthByte Group for all their ~~kind help~~[assistance](#), as well as the University of Sydney for supporting open source [and open access](#) research.

15

## References

- Algeo, T.J., Berner, R.A., Maynard, J.B. and Schekler, S.E.: Late Devonian oceanic anoxic events and biotic crises: “Rooted” in the evolution of vascular land plants?, *GSA Today*, 5, 64-66, 1995.
- Anagnostou, E., John, E. H., Edgar, K. M., Foster, G. L., Ridgwell, A., Inglis, G. N., Pancost, R.D., Lunt,  
20 D.J., Pearson, P. N.: Changing atmospheric CO<sub>2</sub> concentration was the primary driver of early Cenozoic climate, *Nature*, 533,7603, 380-384, 2016.
- Belcher, C. M., and Mander, L.: Catastrophe: Extraterrestrial impacts, massive volcanism, and the biosphere, in *The Future of the World’s Climate*, edited by A. Henderson-Sellers and K. McGruffie, 463–485, Elsevier, Amsterdam, 2012.

- Berner, R. A., and Caldeira, K.: The need for Mass balance and feedback in the geochemical carbon cycle, *Geology*, 25, 955-956, 1997.
- Berner, R. A., and Kothavala, Z.: GEOCARB III: a revised model of atmospheric CO<sub>2</sub> over Phanerozoic time, *American Journal of Science*, 301, 182-204, 2001.
- 5 Berner, R. A.: *The Phanerozoic Carbon Cycle: CO<sub>2</sub> and O<sub>2</sub>*, Oxford University Press, 2004.
- Berner, R.A.: GEOCARBSULF: A combined model for Phanerozoic atmospheric O<sub>2</sub> and CO<sub>2</sub>, *Geochimica et Cosmochimica Acta*, 70, 23, 5653-5664, 2006.
- Boyden, J. A., Müller, R. D., Gurnis, M., Torsvik, T. H., Clark, J. A., Turner, M., Ivey-Law, H., Watson, R. J., and Cannon, J. S.: Next-generation plate-tectonic reconstructions using GPlates, *Geoinformatics: cyberinfrastructure for the solid earth sciences*, 9, 5-114, 2011.
- 10 Burton, M. R., Sawyer, G. M., and Granieri, D.: Deep carbon emissions from volcanoes, *Rev. Mineral. Geochem*, 75, 323-354, 2013.
- Caballero, R., and Huber, M.: State-dependent climate sensitivity in past warm climates and its implications for future climate projections, *Proceedings of the National Academy of Sciences*, 110, 15 14162-14167, 2013.
- Cao, W., Lee, C-T. A., Lackey, J.S.: Episodic nature of continental arc activity since 750 Ma: A global compilation, *Earth and Planetary Science Letters*, 461, 85-95, 2016.
- Carter, L. B., and Dasgupta, R.: Hydrous basalt–limestone interaction at crustal conditions: Implications for generation of ultracalcic melts and outflux of CO<sub>2</sub> at volcanic arcs, *Earth and Planetary Science Letters*, 427, 202-214, 2015.
- 20 Cohen, K., Finney, S., Gibbard, P., and Fan, J.-X.: The ICS international chronostratigraphic chart, *Episodes*, 36, 199-204, 2013.
- Domeier, M., and Torsvik, T. H.: Plate tectonics in the late Palaeozoic, *Geoscience Frontiers*, 5, 303-350, 2014.
- 25 Doss, S., Zahirovic, S., Müller, D. and Pall, J.: DCO Modelling Of Deep Time Atmospheric Carbon Flux from Subduction Zone Interactions: Plate Models and Minor Edits, <http://doi.org/10.5281/zenodo.154001>, 2016.
- EarthByte Group: GPlates 1.5, Sydney, Australia <http://www.gplates.org/download.html>, 2015.

- ESRI: Release 10, Documentation Manual. Redlands, CA, Environmental Systems Research Institute, 2011.
- Fischer, T. P.: Fluxes of volatiles (H<sub>2</sub>O, CO<sub>2</sub>, N<sub>2</sub>, Cl, F) from arc volcanoes, *Geochemical Journal*, 42, 21-38, 2008.
- 5 Golonka, J. and Kiessling, W.: Phanerozoic time scale and definition of time slices, in: *Phanerozoic Reef Patterns*, Kiessling, W., Flugel, E. and Golonka, J. (eds), SEPM (Society for Sedimentary Geology) Special Publication 72, 11-29, 2002.
- [Gonzalez, C., Gorczyk, W., and Gerya, T.: Decarbonation of subducting slabs: Insight from petrological–thermomechanical modeling, \*Gondwana Research\*, 36, 314-332, 2016.](#)
- 10 Grinsted, A., Moore, J. C., and Jevrejeva, S.: Application of the cross wavelet transform and wavelet coherence to geophysical time series, *Nonlinear processes in geophysics*, 11, 561-566, 2004.
- [Grotzinger, J. P., and James, N. P.: Precambrian carbonates: evolution of understanding, \*SEPM Special Publication\* 6, 3-20, 2000.](#)
- [Gurnis, M., Turner, M., Zahirovic, S., DiCaprio, L., Spasojevic, S., Müller, R., Boyden, J., Seton, M.,](#)
- 15 [Manea, V., and Bower, D.: Plate Tectonic Reconstructions with Continuously Closing Plates, \*Computers & Geosciences\*, 38, 35-42, 2012.](#)
- IPCC: Climate Change 2013: The Physical Science Basis. Contribution of Working Group I to the Fifth Assessment Report of the Intergovernmental Panel on Climate Change, Cambridge University Press, Cambridge, United Kingdom and New York, NY, USA, 1535 pp., 2013.
- 20 Jagoutz, O., Macdonald, F. A., and Royden, L.: Low-latitude arc–continent collision as a driver for global cooling, *Proceedings of the National Academy of Sciences*, 113, 4935-4940, 2016.
- Johnston, F. K., Turchyn, A. V., and Edmonds, M.: Decarbonation efficiency in subduction zones: Implications for warm Cretaceous climates, *Earth and Planetary Science Letters*, 303, 143-152, 2011.
- Keleman, P., and Manning, C.: Reevaluating carbon fluxes in subduction zones, what goes down, mostly
- 25 comes up. *PNAS* 112, E3997–E4006, 2015.
- Kent, D. V., and Muttoni, G.: Equatorial convergence of India and early Cenozoic climate trends, *Proceedings of the National Academy of Sciences*, 105, 16065-16070, 2008.

- Kent, D. V., and Muttoni, G.: Modulation of Late Cretaceous and Cenozoic climate by variable drawdown of atmospheric pCO<sub>2</sub> from weathering of basaltic provinces on continents drifting through the equatorial humid belt, *Climate of the Past*, 9, 525-546, 2013.
- Kerrick, D. M.: Present and past nonanthropogenic CO<sub>2</sub> degassing from the solid Earth, *Reviews of Geophysics*, 39, 565-585, 2001.
- Kerrick, D., and Connolly, J.: Metamorphic devolatilization of subducted oceanic metabasalts: implications for seismicity, arc Magmatism and volatile recycling, *Earth and Planetary Science Letters*, 189, 19-29, 2001.
- Kiessling, W., Flügel, E., and Golonka, J.: Fluctuations in the carbonate production of Phanerozoic reefs, *Geological Society, London, Special Publications*, 178, 191-215, 2000.
- Kiessling, W., Flügel, E., and Golonka, J.: Patterns of Phanerozoic carbonate platform sedimentation, *Lethaia*, 36, 195-225, 2003.
- Kump, L. R., Brantley, S. L., and Arthur, M. A.: Chemical weathering, atmospheric CO<sub>2</sub>, and climate, *Annual Review of Earth and Planetary Sciences*, 28, 611-667, 2000.
- Lau, K., and Weng, H.: Climate signal detection using wavelet transform: How to make a time series sing, *Bulletin of the American Meteorological Society*, 76, 2391-2402, 1995.
- Lee, C. T. A., Lackey, J. S.: Global continental arc flare-ups and their relation to long-term greenhouse conditions, *Elements*, 11, 125-130, 2015.
- Lee, C.-T. A., Shen, B., Slotnick, B. S., Liao, K., Dickens, G. R., Yokoyama, Y., Lenardic, A., Dasgupta, R., Jellinek, M., and Lackey, J. S.: Continental arc–island arc fluctuations, growth of crustal carbonates, and long-term climate change, *Geosphere*, 9, 21-36, 2013.
- Lee, H., Muirhead, J. D., Fischer, T. P., Ebinger, C. J., Kattenhorn, S. A., Sharp, Z. D., and Kianji, G.: Massive and prolonged deep carbon emissions associated with continental rifting, *Nature Geoscience*, 2016.
- 25 [Lenardic, A., Moresi, L., Jellinek, A., O'Neill, C., Cooper, C.M. and Lee, C.T.: Continents, supercontinents, mantle thermal mixing, and mantle thermal isolation: Theory, numerical simulations and laboratory experiments, \*Geochem. Geophys. Geosyst.\*, 12, Q10016, doi:10.1029/2011GC003663, 2011.](#)

~~Lenardic, A., Jellinek, A., Foley, B., O'Neill, C., and Moore, W.: Climate-tectonic coupling: Variations in the mean, variations about the mean, and variations in mode, *Journal of Geophysical Research: Planets*, 2016.~~

- Matthews, K. J., Maloney, K. T., Zahirovic, S., Williams, S. E., Seton, M., and Müller, R. D.: Global plate boundary evolution and kinematics since the late Palaeozoic, *Global and Planetary Change*, 146, 226-250, <http://dx.doi.org/10.1016/j.gloplacha.2016.10.002>, 2016.
- McCourt, W., Crow, M., Cobbing, E., and Amin, T.: Mesozoic and Cenozoic plutonic evolution of SE Asia: evidence from Sumatra, Indonesia, Geological Society, London, Special Publications, 106,1, 321-335, 1996.
- 10 McKenzie, N. R., Horton, B. K., Loomis, S. E., Stockli, D. F., Planavsky, N. J., and Lee, C. T.: Continental arc volcanism as the principal driver of icehouse-greenhouse variability, *Science (New York, N.Y.)*, 352, 444-447, [10.1126/science.aad5787](https://doi.org/10.1126/science.aad5787), 2016.
- Merdith, A.S., Collins, A.S., Williams, S.E., Pisarevsky, S., Foden, J.D., Archibald, D.B., Blades, M.L., Alessio, B.L., Armistead, S., Plavsa, D., Clark, C. and Muller, R.D.: A full-plate global reconstruction of Neoproterozoic, *Gondwana research*, 50, 84-134, 2017.
- 15 Müller, R. D., Seton, M., Zahirovic, S., Williams, S. E., Matthews, K. J., Wright, N. M., Shephard, G. E., Maloney, K., Barnett-Moore, N., and Hosseinpour, M.: Ocean basin evolution and global-scale plate reorganization events since Pangea breakup, *Annual Review of Earth and Planetary Sciences*, 44, 107-138, 2016.
- 20 Park, J., and Royer, D. L.: Geologic constraints on the glacial amplification of Phanerozoic climate sensitivity, *American Journal of Science*, 311, 1-26, 2011.
- Prokoph, A., and El Bilali, H.: Cross-wavelet analysis: a tool for detection of relationships between palaeoclimate proxy records, *Mathematical geosciences*, 40, 575-586, 2008.
- Rea, D. K., and Ruff, L. J.: Composition and Mass flux of sediment entering the world's subduction zones: implications for global sediment budgets, great earthquakes, and volcanism, *Earth and Planetary Science Letters*, 140, 1-12, 1996.
- 25 Ridgwell, A., and Zeebe, R.: The role of the global carbonate cycle in the regulation and evolution of the Earth system, *Earth and Planetary Science Letters*, 234, 299-315, [10.1016/j.epsl.2005.03.006](https://doi.org/10.1016/j.epsl.2005.03.006), 2005.



- Royer, D. L.: CO<sub>2</sub>-forced climate thresholds during the Phanerozoic, *Geochimica et Cosmochimica Acta*, 70, 5665-5675, 2006.
- Scotese, C. R.: PALAEOMAP PalaeoAtlas for GPlates and the PalaeoData Plotter Program, PALAEOMAP Project, <http://www.earthbyte.org/palaeomap-palaeoatlas-for-gplates>, 2016.
- 5 Siebert, L., and Simkin, T.: *Volcanoes of the world: An illustrated catalog of Holocene volcanoes and their eruptions*, 2014.
- [Seton, M., Müller, R., Zahirovic, S., Gaina, C., Torsvik, T., Shephard, G., Talsma, A., Gurnis, M., Turner, M., Maus, S., and Chandler, M.: Global continental and ocean basin reconstructions since 200 Ma, \*Earth-Science Reviews\*, 113, 212-270, 2012.](#)
- 10 Sundquist, E. T.: Steady- and non-steady-state carbonate-silicate controls on atmospheric CO<sub>2</sub>, *Quaternary Science Reviews*, 10, 283-296, [http://dx.doi.org/10.1016/0277-3791\(91\)90026-Q](http://dx.doi.org/10.1016/0277-3791(91)90026-Q), 1991.
- Torrence, C., and Compo, G. P.: A practical guide to wavelet analysis, *Bulletin of the American Meteorological society*, 79, 61-78, 1998.
- 15 van der Meer, D. G., Zeebe, R. E., van Hinsbergen, D. J., Sluijs, A., Spakman, W., and Torsvik, T. H.: Plate tectonic controls on atmospheric CO<sub>2</sub> levels since the Triassic, *Proceedings of the National Academy of Sciences*, 111, 4380-4385, 2014.
- Walker, J. C., Hays, P., and Kasting, J. F.: A negative feedback mechanism for the long-term stabilization of Earth's surface temperature, *Journal of Geophysical Research: Oceans*, 86, 9776-9782, 1981.
- 20 Wessel, P., Smith, W.H.F., Scharroo, R., Luis, J.F. and Wobbe, F.: GMT 5.2.1., SOEST, Dept. of Geology & Geophysics, Honolulu, Hawaii, <http://gmt.soest.hawaii.edu/projects/gmt/wiki/Download>, 2015.
- Whittaker, J.M., Müller, R.D., Sdrolias, M., and Heine, C.: Sunda-Java trench kinematics, slab window formation and overriding plate deformation since the Cretaceous, *Earth and Planetary Science Letters*, 255, 445-457, <http://dx.doi.org/10.1016/j.epsl.2006.12.031>, 2007.
- 25 Winder, S.: *Analog and Digital Filter Design*, Elsevier Science, 2002.
- Zahirovic, S., Matthews, K. J., Flament, N., Müller, R. D., Hill, K. C., Seton, M., and Gurnis, M.: Tectonic evolution and deep mantle structure of the eastern Tethys since the latest Jurassic, *Earth Science Reviews*, 162, 293-337, 2016.